Intercomparison of the ‘R91’ Gaussian Plume Model and the UK Met Office’s Lagrangian Particle NAME III Model in the Context of a Short-duration Release

P Bedwell, J Wellings, S M Haywood, M C Hort*, A R Jones* and D J Thomson*

* MET OFFICE, FITZROY ROAD, EXETER, DEVON EX1 3PB, UK

ABSTRACT

This report compares the predictions of HPA’s application of the ‘R91’ model with those of the UK Met Office’s NAME III model. The study considers a simplified application of NAME and R91 to enable a fair model comparison. The comparison is centred upon analysis of model output generated from a single baseline run for a short duration release of the type often considered in emergency response assessments. Subsequent model runs are performed, scoping a range of model scenarios and commonly modified model input parameters. Differences in the predictions of the two models are investigated and explained. The quantitative assessment of differences in the baseline model output is used as part of a qualitative assessment of observed differences across a range of model runs and their associated output.

There is a disparity (of up to a factor of approximately 3) between time-integrated activity concentrations in air derived using NAME and those derived using R91, most notably in the near-field. R91 is more conservative in its approach, and estimates made by R91 are typically greater than those made by NAME. The cross-wind spread of the plume, vertical spread of the plume and wind-driven advection of the plume are identified as the primary sources of the observed differences between R91 and NAME model output.

Centre for Radiation, Chemical and Environmental Hazards
Chilton, Didcot,
Oxfordshire OX11 0RQ

Approval: July 2011
Publication: November 2011
£21.00
ISBN 978-0-85951-710-2

This work was undertaken under the Environmental Assessment Department's Quality Management System, which has been approved by Lloyd's Register Quality Assurance to the Quality Management Standards ISO 9001:2008 and TickIT Guide Issue 5.5, Certificate No: LRQ 0956546.

Report version 1.0

CONTENTS

1 INTRODUCTION

The HPA (Health Protection Agency) has, for many years[1], used the simple Gaussian Plume Diffusion Model developed by the Working Group on Atmospheric Dispersion (now recognised as the Atmospheric Dispersion Modelling Liaison Committee), Clarke (1979). That report is commonly referred to as NRPB-R91 and the model described in the report is referred to here as 'R91'. HPA applies R91 to describe the atmospheric dispersion of radionuclides across a wide range of applications, including emergency response.

This report compares the predictions of the R91 model (as used for emergency response assessments) with those of NAME III, the UK Met Office's Lagrangian particle model (Numerical Atmospheric-dispersion Modelling Environment), as described by Jones et al (2007). The study considers a simplified application of NAME III and R91 to enable a fair model comparison. The comparison is centred upon analysis of model output generated from a single baseline run for a short duration release of the type often considered in emergency response assessments. Subsequent model runs are performed, scoping a range of model scenarios and commonly modified model input parameters. Differences in the predictions of the two models are investigated and explained. The quantitative assessment of differences in the baseline model output is used as part of a qualitative assessment of observed differences across a range of model runs and their associated output. For simplicity, NAME III is referred to as NAME for the remainder of this report. A summary of the acronyms included in this report can be found in Appendix A.

2 MODEL SUMMARY

2.1 R91 Method

The R91 Gaussian plume model is a simple and robust method of predicting dispersion, although with recognised limitations (Clarke, 1979). This approach has traditionally been used by a number of parties, including HPA, in preference to more complex systems or models due to its simplistic and transparent method and computationally inexpensive approach. R91 is also suitable for applications which require indicative rather than precise output, as is often the case in radiological assessments.

The implementation of R91 in this study includes the R91 Gaussian plume model equation with the inclusion of virtual sources characterising the impact of the ground and atmospheric boundary layer top on activity concentrations in air (Clarke, 1979), as detailed in Appendix B. The implementation also assumes no radioactive decay during the plume passage and does not include plume depletion due to deposition processes;

[1] Prior to 2005, the section of the HPA which undertook radiological assessments was the National Radiological Protection Board (NRPB), which in 2005 became part of the HPA.

this is considered justifiable over the relatively short temporal and spatial scales typical in emergency response assessments for radiological incidents. Dry deposition is modelled by means of deposition velocities (Jones, 1983). Wet deposition is modelled using two empirical enhancement factors of dry deposition, representing light and heavy rainfall. The method uses discrete pre-calculated time integrated activity concentrations in air per unit release for a 30 minute release duration, for Pasquill Stability Categories (A-G), a range of release heights (0-200 m) and a range of distances downwind (0-100 km). To account for a range of release durations, time integrated activity concentrations in air are scaled by a release duration correction factor (Clarke, 1979). Output is calculated for a pre-defined source term. Note that 'R91' as discussed here refers to the form of R91 and associated assumptions implemented in HPA's emergency assessment tool, which does not strictly conform to the NRPB-R91 report (Clarke, 1979) and subsequent series of NRPB board reports (including Jones, 1981 and Jones, 1983), notably a simplified method used to model wet deposition.

2.2 NAME

NAME is a Lagrangian particle dispersion model developed by the UK Met Office and designed to predict atmospheric dispersion and deposition of gases and particulates (Jones et al, 2007). In this report, particles are used to describe dispersion; puff modelling in NAME may be considered in a future intercomparison. The mean flow or advection of a particle is determined by the flow information, primarily the wind velocity, detailed in the required meteorological data. Diffusion is described by random walk (Monte Carlo) processes, determined by the turbulent velocity. Each particle carries a mass or activity of one or more pollutant species and evolves by various physical and chemical processes during its lifespan. In the context of a radiological release the pollutant species are radionuclides or radionuclide groups. A box-averaging scheme is used to derive activity concentrations in air from particle activities. The dry deposition scheme in NAME uses a deposition velocity, whereby the flux of a pollutant to the ground is proportional to the concentration and deposition velocity. The wet deposition scheme in NAME uses scavenging coefficients (a function of the precipitation rate, type of precipitation and type of deposition process). The mass by which each particle is depleted is dependent upon the mass (in this case the activity concentration), time and scavenging coefficient. The capabilities of NAME are considerably greater than those used in this study, but to ensure a fair comparison with R91, NAME is applied in a very simplistic manner.

3 DESCRIPTION OF THE BASELINE MODEL RUN

Model comparisons between R91 and NAME are centred upon the analysis of model output generated from a single baseline run, representing a short duration release. A description of the baseline model parameter values are detailed in Table 1. The model input parameters are hypothetical but representative of a possible accidental release. The meteorological data assumed equate to the most commonly observed Pasquill stability category in the UK, stability category D, as defined by Clarke (1979). Single site meteorological data are used rather than NWP (Numerical Weather Prediction) meteorological data. A single radionuclide, ^{137}Cs, is considered.

The baseline model run assumes a zero value for deposition velocity, forcing NAME to exclude plume depletion and thus ensuring consistency with R91.

Table 1 Parameters applied in the baseline model run

Parameter	Baseline value
Source term (^{137}Cs)	1.0 10^{16} Bq
Release duration	1 hour
Release height (stack)	10 m
Plume rise (effective release height)	None (the release height is the baseline 10 m)
Pasquill meteorological stability category	D
Mixing layer depth	800 m
Surface sensible heat flux	0 W m^{-2}
Wind speed (in NAME, wind speed at 10m above ground)	5 m s^{-1}
Wind direction	Steady state (direction arbitrary)
Particle size	100% 1 µm AMAD
Radioactive decay	No
Dry deposition velocity	0 m s^{-1}
Rain-out/washout coefficient	No rain
Roughness length	0.3 m (typical rural land)
Terrain and building effects	None

The release was assumed to be uniform over the entire duration and assumed to be from a point source.

NAME version 5.3 was used for all NAME model runs in this study. Many of the enhanced features of NAME were not applied in this study [1].

4 QUANTITATIVE ASSESSMENT OF THE DIFFERENCES OBSERVED BETWEEN NAME AND R91 OUTPUT FOR A BASELINE MODEL RUN

NAME and R91 baseline model runs, based on the assumptions summarised in Table 1, were undertaken to estimate time integrated activity concentrations in air (TIACs) as a function of distance downwind. These results are summarised in Table 2. There is a

[1] The near source scheme was not used in NAME; the velocity memory time and inhomogeneous time were both set to zero. The turbulent and meander schemes were applied for all NAME model runs. For further details see Section 6.

disparity (of up to a factor of 3.4) between those plume centre line (PCL) TIACs derived using NAME and those derived using R91, most notably at one kilometre downwind from the release (Table 2 and Figure 1 to Figure 3). In the range 1 to 40 km downwind all TIACs estimated by R91 are greater than that estimated by NAME. The differences observed in Table 2 are indicative of a discrepancy but do not reflect the totality of the differences between the models. This is because there exist multiple factors responsible for the difference in TIACs, some of which act to counterbalance and obscure the magnitude of the disparity. These are discussed below.

Table 2 Ground level time integrated activity concentrations in air (Bq s m^{-3}) as a function of distance on PCL

	1 km	2 km	5 km	10 km	20 km	40 km
NAME baseline model run	$3.8\ 10^{10}$	$1.5\ 10^{10}$	$4.4\ 10^{9}$	$1.8\ 10^{9}$	$7.3\ 10^{8}$	$2.9\ 10^{8}$
R91 baseline model run	$1.3\ 10^{11}$	$4.1\ 10^{10}$	$9.2\ 10^{9}$	$3.1\ 10^{9}$	$1.1\ 10^{9}$	$4.2\ 10^{8}$

Greater variability between TIACs estimated by R91 and NAME than that demonstrated in Table 2 is found off the PCL, at least for those model run assumptions and downwind distances considered here. It is evident from Figure 1 that at 1 km downwind and 0.5 km off the PCL, estimated TIACs may differ by a factor of 100. The implications of such a difference could be significant if using such output to estimate dose; however, a dose assessment often focuses on the most exposed population, which tends to reside on or relatively close to the PCL, where differences are less pronounced. It is recognised that relatively small differences in σ_y and σ_z result in increasing fractional differences in concentration at increasing distances into the tail of the plume. Furthermore, the concentrations themselves reduce significantly in the tail and therefore large fractional errors may not be important. However, it is important to consider differences off the plume centre line, where the population at most risk may reside.

Differences in the cross-wind spread of the plume, vertical spread of the plume and wind-driven advection of the plume are potential factors contributing to the observed differences between R91 and NAME model concentration outputs. In the remainder of this chapter each potential cause is considered individually and finally all three are considered cumulatively, to analyse the differences observed between R91 and NAME baseline model run estimates, as detailed in Table 2.

4.1 The cross-wind spread of the plume

The cross-wind spread of the plume is described by the standard deviation of the cross-wind plume profile (σ_y) in R91. The standard deviation of the cross-wind plume profile is expressed by two terms; a turbulent diffusion term (based on Pasquill's Diffusion Curves derived using empirical data, notably from the Prairie Grass experiments (Barad, 1958)) as detailed in Gifford (1968), and a wind direction fluctuation term (based on empirical data) as detailed in Moore (1976). The turbulent diffusion term is a function of Pasquill stability category and distance downwind. The wind direction fluctuation term is a function of release duration, distance downwind and wind speed at a height of 10 m. NAME does not describe the spread of the plume directly in terms of a standard deviation of the cross-wind plume profile. Instead, it is determined by meteorological data, which, amongst other things, describes the mean flow of the particles, and by random walk techniques used to describe the turbulent motion of the particles (Maryon et al, 1999). However, cross-wind profiles of TIACs were estimated by NAME at 1, 2, 5, 10, 20 and 40 km downwind, from which estimates of σ_y were made, as detailed in Appendix C.

Table 3 Standard deviation of the cross-wind plume profile, σ_y (m), as a function of distance downwind

	1 km	2 km	5 km	10 km	20 km	40 km
NAME baseline model run	150	260	520	870	1500	2500
R91 baseline model run	110	210	520	1000	2000	3700

At distances less than 5 km downwind the spread of a plume in the y axis is greater when modelled by NAME than by R91 (Table 3 and Figure 1), implying a greater degree of mixing modelled within NAME in the cross-wind direction at relatively short distances from the release (for the baseline model run conditions and distances downwind considered here). Conversely, at distances greater than 5 km downwind the spread of a plume in the y axis is less when modelled by NAME than by R91, implying a lesser degree of mixing modelled within NAME in the cross-wind direction at relatively large distances from the release. In all cases the difference in σ_y estimated by the two models is less than a factor of 1.5.

The inflection in the NAME tail in Figure 2 is almost certainly the result of statistical noise.

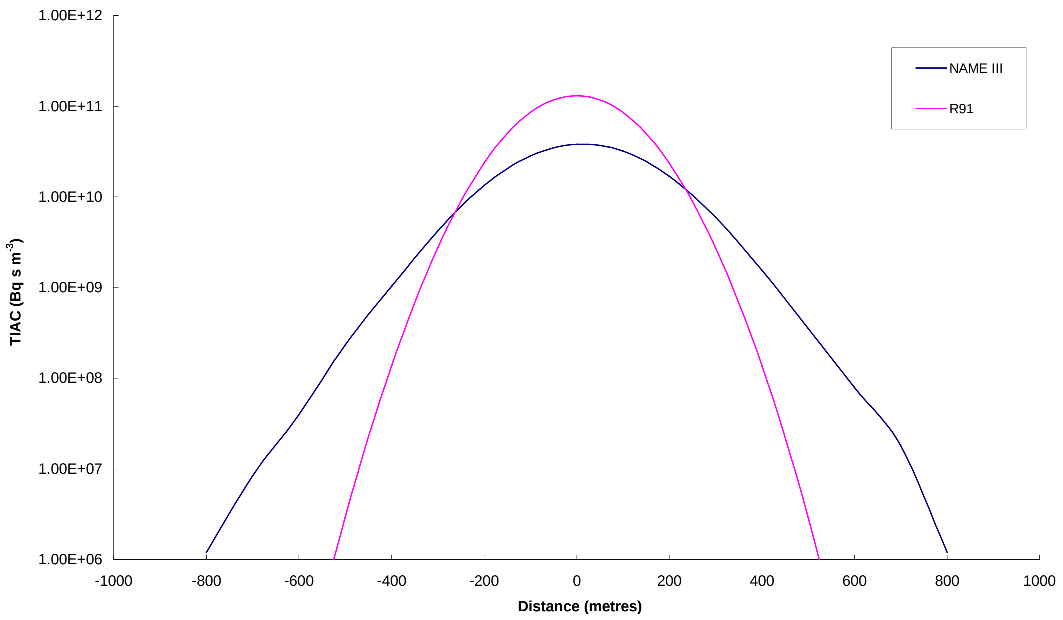

Figure 1 Cross-wind plume profile of the time integrated activity concentrations in air at 1 km downwind

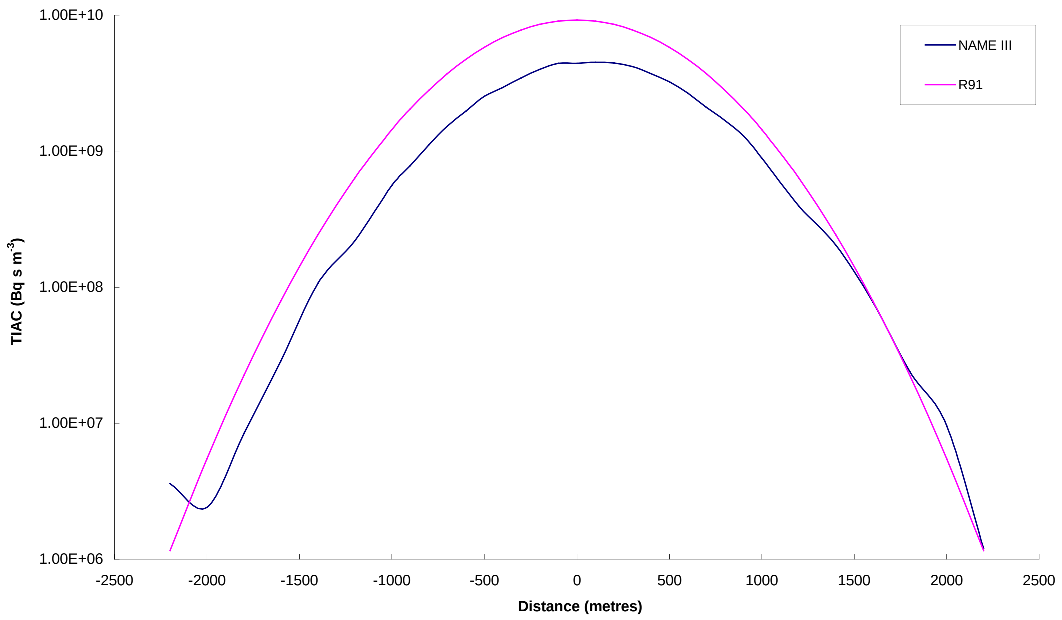

Figure 2 Cross-wind plume profile of the time integrated activity concentrations in air at 5 km downwind

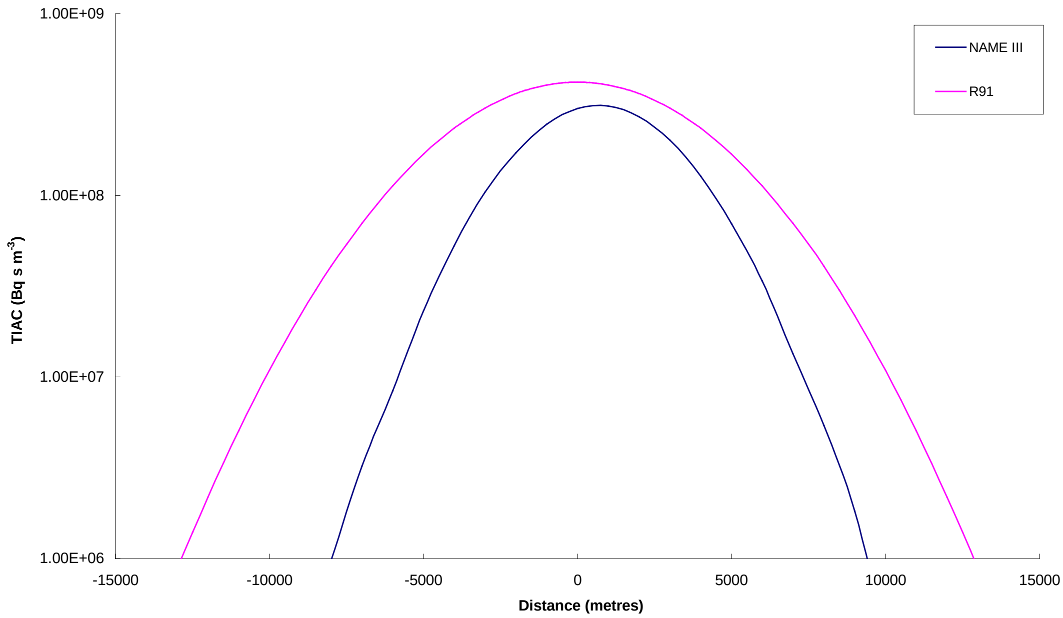

Figure 3 Cross-wind plume profile of the time integrated activity concentrations in air at 40 km downwind

To investigate the contribution that differences in the cross-wind plume profile (σ_y) make to the difference in the predictions of NAME and R91, a modified R91 run using σ_y derived from NAME model output (Table 4) was undertaken. The differences in TIACs between this run and the NAME baseline run are less than a factor of 2.5 at all distances downwind. This improved agreement between NAME and R91-estimated TIACs at distances of less than 5 km downwind indicates that the different method used in the two models to describe the cross-wind spread of the plume is partially but not entirely responsible for the differences in the observed model output. At distances greater than 5 km downwind the difference between NAME- and R91-estimated TIACs is amplified, suggesting an alternative explanation for the observed differences between R91 and NAME model output at such distances.

Table 4 Ground level time integrated activity concentrations in air (Bq s m^{-3}) as a function of distance downwind, for a modified R91 cross-wind plume profile based on NAME model output

	1 km	2 km	5 km	10 km	20 km	40 km
NAME baseline model run	$3.8\ 10^{10}$	$1.5\ 10^{10}$	$4.4\ 10^{9}$	$1.8\ 10^{9}$	$7.3\ 10^{8}$	$2.9\ 10^{8}$
R91 baseline model run, modified by σ_y derived from the NAME baseline model run	$9.2\ 10^{10}$	$3.3\ 10^{10}$	$9.1\ 10^{9}$	$3.6\ 10^{9}$	$1.5\ 10^{9}$	$6.2\ 10^{8}$

4.2 The vertical spread of the plume

The vertical spread of the plume is described by the standard deviation of the unreflected vertical plume profile ($\sigma_{z,unreflected}$) in R91 (based on Smith (1973)). The standard deviation of the vertical plume profile is a function of the atmospheric stability, downwind distance and ground roughness. The spread of a plume in NAME is not described directly in terms of the standard deviation of the vertical plume profile. Instead, it is determined by meteorological data, which, amongst other things, describes the mean flow of the particles, and by random walk techniques used to describe the turbulent motion of the particles (Maryon et al, 1999). Vertical profiles of TIACs were estimated by NAME at 1, 2, 5, 10, 20 and 40 km downwind, from which estimates of the standard deviation of the reflected vertical plume profile ($\sigma_{z,reflected}$) were made, as detailed in Appendix C.

Table 5 Standard deviation of the vertical plume profile, σ_z (m), as a function of distance downwind

	1 km	2 km	5 km	10 km	20 km	40 km
NAME baseline model run	48	65	98	130	180	230
R91 baseline model run	27 (44)	44 (73)	80 (130)	120 (200)	178 (300)	250 (410)

R91 baseline model run output detailed in brackets are values of σ_z taken directly from Clarke (1979), see text for details

The principal R91 values in Table 5 (the values not in brackets) assume a reflected vertical plume profile off the ground, but not off the top of the boundary layer (as detailed in Appendix C), to enable fair comparison with NAME derived $\sigma_{z,reflected}$ values. The R91 values in brackets ($\sigma_{z,unreflected}$) are taken directly from Clarke (1979) but are not comparable with NAME $\sigma_{z,reflected}$ values because they refer to the unreflected plume and do not account for the impact of the ground (nor the boundary layer top) on the spread of the plume. To put the values in Table 5 into context, for a uniform distribution across the (800 m deep) boundary layer, the estimated value of σ_z is 230 m (for details see Appendix D).

It is evident (see Table 5, Figure 4 and Figure 5) that for the baseline model run at distances less than 20 km, $\sigma_{z,reflected}$ in NAME is greater than $\sigma_{z,reflected}$ in R91, implying a greater degree of mixing in the vertical cross section at the majority of downwind distances considered here. The true extent of the difference in vertical mixing at relatively small distances from the release is demonstrated in Figure 4. Over the lowest 200 m of the boundary layer the TIACs estimated by NAME vary by less than a factor of 25. In contrast the TIACs estimated by R91 vary by more than a factor of 10,000 over the same boundary layer depth. This is indicative of the greater mixing of the plume in NAME; however, it is recognised that at increasing distances into the tail of the plume, the associated TIACs become more sensitive to error. Only at 40 km downwind (for those distances considered here) is $\sigma_{z,reflected}$ in NAME less than in R91 (see Table 4 and Figure 6), implying less mixing in the vertical cross section in NAME at relatively large distances from the release. In all cases the difference in $\sigma_{z,reflected}$ (along the PCL) between the two models is less than a factor of 2.

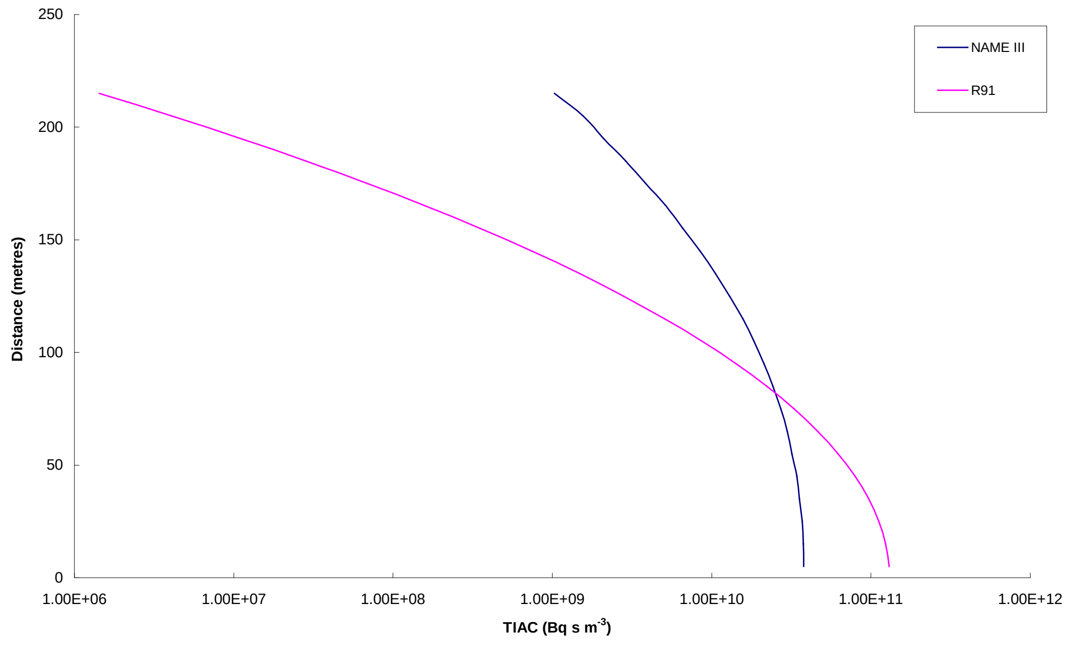

Figure 4 Vertical plume profile of the time integrated activity concentrations in air at 1 km downwind

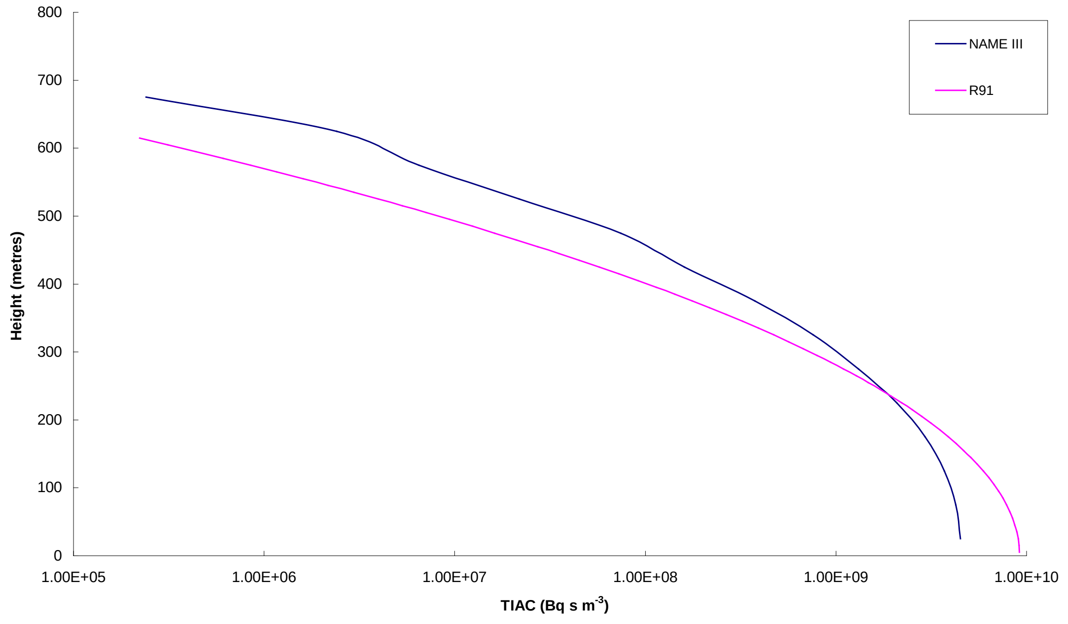

Figure 5 Vertical plume profile of the time integrated activity concentrations in air at 5 km downwind

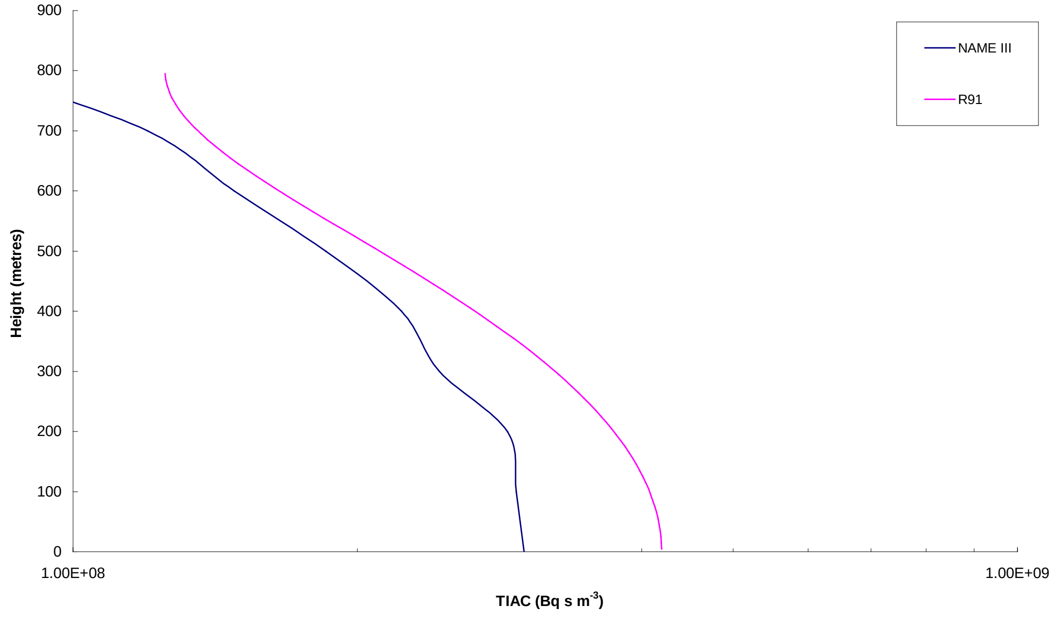

Figure 6 Vertical plume profile of the time integrated activity concentrations in air at 40 km downwind

To investigate the contribution that differences in the standard deviation of the vertical plume profile (σ_z) make to the difference in the predictions of NAME and R91, a modified R91 run was undertaken (Table 6). The modified R91 run used $\sigma_{z,unreflected}$ derived values from NAME model output, scaled from their original $\sigma_{z,reflected}$ form, as detailed in Appendix C. The differences in TIACs between this run and the NAME baseline run are less than a factor of 2 at all distances downwind. The improved agreement between the NAME and R91 TIACs at all distances considered (barring 40 km downwind, where a marginal divergence in estimated TIACs is observed) indicates that the different method used to describe the vertical spread of the plume is partially but not entirely responsible for the differences in the observed model output.

Table 6 Ground level time integrated activity concentrations in air (Bq s m^{-3}) as a function of distance downwind, for a modified R91 vertical plume profile based on NAME model output

	1 km	2 km	5 km	10 km	20 km	40 km
NAME baseline model run	$3.8\ 10^{10}$	$1.5\ 10^{10}$	$4.4\ 10^{9}$	$1.8\ 10^{9}$	$7.3\ 10^{8}$	$2.9\ 10^{8}$
R91 baseline model run, modified by σ_z derived from the NAME baseline model run	$7.4\ 10^{10}$	$2.8\ 10^{10}$	$7.5\ 10^{9}$	$2.8\ 10^{9}$	$1.1\ 10^{9}$	$4.6\ 10^{8}$

It is evident from Sections 4.1 and 4.2 that in spite of the application in R91 of both cross-wind spread and vertical spread consistent with NAME, R91 systematically estimates TIACs greater than NAME at relatively large distances downwind, most notably 40 km.

4.3 Advection of a plume downwind

NAME and R91 differ in how they model wind speed as a function of height. R91 assumes a single wind speed typically at a height of 10 metres above ground level. The approach implemented in NAME is more representative of the entire boundary layer in that it considers a wind profile, whereby wind speed typically increases with height as a result of the decreasing influence of the earth's relatively rough surface. Thus, with increasing distance from the ground the plume is (typically) advected downwind at increasing speeds, which acts to reduce the activity concentrations in air at ground level in NAME. Specifically, the wind field derived in NAME (from single site met) applies the same approach as ADMS (CERC, 2010). If A is the boundary layer depth and L_{MO} is the Monin-Obukhov length, then in convective conditions, where $A/L_{MO}<0$, Panofsky and Dutton (1984) is used to derive the profile of the mean wind. In stable-neutral conditions, where $A/L_{MO}=>0$, van Ulden and Holtslag (1985) is used to derive the profile of the mean wind.

R91 considers only a single wind speed across the vertical profile of the plume, thus making it difficult to modify the R91 baseline model run such that it is representative of the range of wind speeds (as a function of height) which advect a plume in NAME. However, the mean wind speed through the depth of the plume, $\bar{u}$, is likely to be more representative of the NAME approach than the application of a wind speed at 10 m (as in R91). Therefore, in an attempt to compare the two approaches the NAME baseline model run mean wind speed through the depth of the plume has been estimated and applied to R91.

The height of the average wind speed is assumed to be $0.56\bar{z}$ (Pasquill and Smith, 1983), where $\bar{z}$ is the mean height of the plume. A widely used formula for determining wind speed at different heights is the log-law (Clarke, 1979), detailed in Equation 1, where u(z) is the wind speed (m s^{-1}) as a function of height (m), u_* is the friction velocity (m s^{-1}), k is von Karman's constant, z is the height (m) and z_o is the ground roughness length (m). The formula is appropriate for neutral boundary layers, as considered here.

$$u(z) = \frac{u_*}{k} \ln \frac{z}{z_o}$$ **Equation 1**

Vertical profiles of NAME derived TIACs at 1, 2, 5, 10, 20 and 40 km downwind were used to determine $\bar{z}$ and thus, with the aid of Equation 1, $\bar{u}$. It is estimated that the mean wind speeds across the extent of the boundary layer occupied by the plume in NAME are 1.3, 1.4, 1.5, 1.6, 1.7 and 1.8 times greater than u_{10} assumed in R91 baseline model runs, at 1, 2, 5, 10, 20 and 40 km downwind, respectively. It is recognised that this approach will overemphasise the effect at all distances downwind, more significantly at larger distances. For example, applying a correction factor of 1.8 (at 40 km) will overemphasise the effect as the plume only reaches this vertical extent after 40 km (whereas the approach will assume that the plume is advected with this elevated wind speed throughout). However, the approach can still demonstrate the likely effect.

Table 7 Ground level time integrated activity concentrations in air (Bq s m^{-3}) as a function of distance downwind, for modified advection of the plume in R91 based on NAME model output

	1 km	2 km	5 km	10 km	20 km	40 km
NAME baseline model run	$3.8\ 10^{10}$	$1.5\ 10^{10}$	$4.4\ 10^{9}$	$1.8\ 10^{9}$	$7.3\ 10^{8}$	$2.9\ 10^{8}$
R91 baseline model run, modified by $\bar{u}$, derived from the NAME baseline model run	$1.1\ 10^{11}$	$3.3\ 10^{10}$	$7.0\ 10^{9}$	$2.3\ 10^{9}$	$7.8\ 10^{8}$	$2.9\ 10^{8}$

The TIACs estimated by R91 and presented in Table 7 account for the dependency of σ_y (notably σ_{yw}, the component of σ_y due the fluctuations in the wind direction) on u (Clarke, 1979), as well as the direct dependency on the reciprocal of u. Improved agreement in NAME and R91 TIACs is minimal relatively close to the source of the release (of the order of 1 km downwind). However, at tens of kilometres from the release, estimated TIACs from the two models are in very good agreement. This result is plausible, as the differential in wind speed with height is likely to significantly affect ground level activity concentrations in air only when the plume has significant vertical extent, which in turn is increasingly likely at greater distances downwind. Improved agreement between NAME and R91 TIACs at increasing distances downwind indicates that the different method used to describe the advection of a plume downwind is partially but not entirely responsible for the differences in the observed model output.

4.4 The combined impact of plume spreads and advection on model variation

The cross-wind spread of the plume, vertical spread of the plume and wind-driven advection of the plume are considered cumulatively, in an effort to explain the differences in NAME and R91 model output for a pre-defined baseline model run.

Table 8 Ground level time integrated activity concentrations in air (Bq s m^{-3}) as a function of distance downwind, for a modified cross-wind and vertical plume profile and for modified advection of the plume in R91 based on NAME model output

	1 km	2 km	5 km	10 km	20 km	40 km
NAME baseline model run	$3.8\ 10^{10}$	$1.5\ 10^{10}$	$4.4\ 10^{9}$	$1.8\ 10^{9}$	$7.3\ 10^{8}$	$2.9\ 10^{8}$
R91 baseline model run	$1.3\ 10^{11}$	$4.1\ 10^{10}$	$9.2\ 10^{9}$	$3.1\ 10^{9}$	$1.1\ 10^{9}$	$4.2\ 10^{8}$
R91 baseline model run, modified by σ_y, σ_z and $\bar{u}$, derived from the NAME baseline model run	$3.9\ 10^{10}$	$1.6\ 10^{10}$	$4.9\ 10^{9}$	$2.0\ 10^{9}$	$8.4\ 10^{8}$	$3.8\ 10^{8}$

The difference in estimates of TIAC are less than a factor of 1.4 at all distances downwind (considered here) for the NAME baseline model run compared to a modified R91 baseline model run, accounting for σ_y, σ_z and $\bar{u}$, derived using NAME model output (Table 8). The agreement between model output is stronger relatively close to the source of the release, which suggests that at relatively small distances downwind (of the order of a few kilometres), differences in NAME and R91 TIACs can be explained entirely by the difference in the methods used to describe the cross-wind spread of the plume, the vertical spread of the plume and the advection of a plume downwind. At relatively large distances downwind the agreement is somewhat less robust. It is likely that at 40 kilometres downwind the observed difference in the TIACs estimated by the NAME baseline model run and the modified R91 baseline model run is due to further discrepancies in σ_z. The modified R91 baseline model run was tailored to account for σ_z derived using NAME model output. In the derivation of a suitable σ_z for R91 from NAME model output, there is a need to account for the fact that R91 requires as input a value of σ_z which is a measure of the plume width before reflections off the ground and the boundary layer top are applied. In calculating σ_z from NAME model output, reflections off the ground were accounted for, but reflections off the boundary layer top were not. Thus the magnitude of the revised NAME σ_z values should be larger than estimated here, especially at large distances downwind where the plume fills the boundary layer and reflections off the boundary layer top become significant. Larger values of σ_z imply lower TIACs, suggesting a better agreement between the NAME baseline model run and the modified R91 baseline model run than observed in Table 8, more especially at larger distances downwind.

In the near field (ie, at 1 km downwind), differences in σ_z contribute most to the differences observed between the NAME and R91 baseline model runs (Figure 7) and u contributes the least. However, at further distances (at around 40 km downwind), u is the major factor in determining the differences observed.

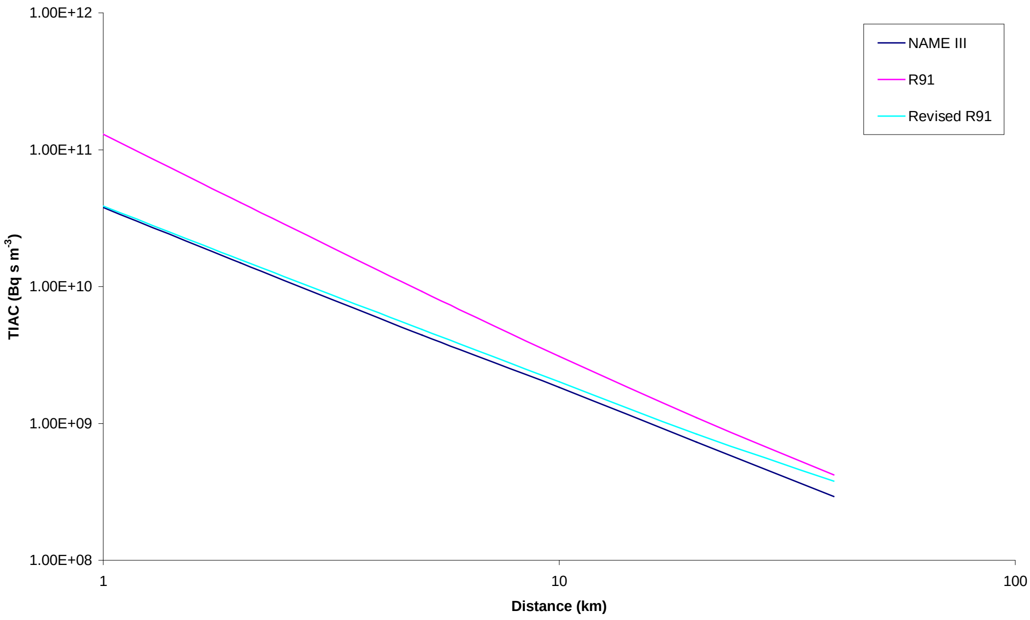

Figure 7 Ground level time integrated activity concentrations in air (Bq s m^{-3}) as a function of distance downwind, for a NAME baseline model run, an R91 baseline model run and an R91 baseline model run modified for σ_y, σ_z and $\bar{u}$, based on NAME model output

4.5 Discussion

It is evident that, for the baseline model run considered here, there exist significant differences between the estimates by NAME and R91 of time integrated activity concentrations in air at ground level on the plume centre line. It is likely, as discussed above, that these differences in model output are due to different methods used within the models to describe the cross-wind spread of the plume, the vertical spread of the plume and the advection of a plume downwind.

It is widely recognised that the velocity of winds adjacent to the earth's surface are greatly affected (typically reduced) by the effects of friction and that with increasing height above the ground the influence of this drag on the velocity of the wind diminishes. When modelling the advection of a plume it is therefore more suitable to consider a vertical wind profile (as considered in NAME) to a single wind speed based at a discrete height above the ground (as assumed by R91). Miller and Hively (1987) state that for short term releases over flat terrain the primary factor in predicting short term concentrations in air seems to be an accurate description of the wind field (assuming accurate source term estimation). Lowles (2002) identified that users of R91-based codes should carefully consider the vertical representation of wind speed input into a Gaussian plume model and recognised potential deficiencies with using a wind speed at a default height of 10 m under all conditions.

The cross-wind spread and vertical spread of the plume in R91 is based on the empirically derived σ_y and σ_z respectively, whereas in NAME the dispersion is modelled statistically by random walk techniques. The former method typically becomes progressively less sound as the conditions under which a plume is dispersing progressively diverge from those upon which the empirical approach was fitted.

Davies and Thomson (1999) recognized that Equation 2 (from Clarke (1979)) underestimates the term σ_{yw}, most notably at low wind speeds. Assuming a one hour averaging time and a wind speed of 5 m s^{-1}, Equation 2 is considered to underestimate σ_{yw} by 1-2 degrees (Davies and Thomson, 1999), resulting in an overestimate of predicted activity concentrations in air. This is likely to be a key factor in the explanation of the larger cross-wind spread of the plume observed in NAME at relatively short distances downwind, as illustrated in Table 3.

In NAME the parameterization of the velocity vector for low-frequency horizontal meandering (Webster and Thomson, 2005) is derived from fixed meander velocity variances and meander Lagrangian timescales, which are estimated from spectra of the resolved motions generated from numerous years worth of Numerical Weather Prediction (NWP) and observed met data for a number of UK sites. The parameterization of meander has generally been found to improve the statistical fit to observations, as demonstrated by the model validation (Ryall and Maryon, 1998) of a former approach recommended by Maryon (1998) against the European Tracer Experiment (ETEX) dataset. It is recognized that the approach recommended by Maryon (1998) and based on wind data from a single site (Cardington, UK) may have limited value elsewhere, especially in regions of differing wind climatology. However the approach recommended by Webster and Thomson (2005) takes greater account of spatial variability and therefore is more reflective of conditions across the UK.

The method applied in NAME to describe the meander of the plume is not proportional to the distance downwind at large distances, contrary to the approach applied in R91 (see Equation 2). Beyond a travel time of about an hour the rate of spread of the plume in NAME reduces relative to the distance downwind to account for the fact that eddies have a finite time scale (ie, the particle meander velocities fluctuate on a time scale of about 1 hour). This is likely to be a key factor in the explanation of the smaller cross-wind spread of the plume observed in NAME at relatively large distances downwind, as illustrated in Table 3.

$$\sigma_{yw} = 0.065x\sqrt{\left(\frac{7T}{u}\right)}$$ **Equation 2**

Where σ_{yw} is the standard deviation of the cross-wind Gaussian plume profile due to fluctuations in wind direction (m), T is the release duration (h), u_{10} is the wind speed at a height of 10 m (m s^{-1}) and x is the distance along the mean wind direction (m).

The relative contributions of σ_{yt} and σ_{yw} are not determined here and therefore it is unclear whether differences in σ_y between the two models are also a result of differences in the methods used to describe turbulent diffusion. R91 describes turbulent diffusion empirically using σ_{yt}. In contrast, NAME applies random walk formulae to determine the turbulent velocity components in both the horizontal and the vertical. NAME considers two schemes, of varying complexity and computational expense, in the estimation of near-source diffusion. The baseline model run assumed the simplified scheme as a result of its suitability for comparison with R91. The horizontal and vertical turbulent velocity variances and Lagrangian timescales are derived from simple diffusion coefficient schemes (K diffusion schemes); constant in the vertical and dependent on travel time in the horizontal (whereby damping of the diffusion coefficient is performed in the near field to reduce the spread of the plume and mimic a more sophisticated scheme). The velocity variances and timescales are then used to estimate turbulent velocity. In this case the turbulence is assumed to be homogeneous. Details of the more advanced near source diffusion scheme, not used in the baseline model run, can be found in Section 6.

NAME's validation against the ETEX dataset (Ryall and Maryon, 1998) is particularly relevant as emphasis was placed on assessing the impact of using a range of advection schemes of varying complexity. The simplistic diffusion scheme, applied in this study, fared well and NAME was found to have performed well for emergency response modelling. NAME successfully predicted the overall spread and timing of the plume across Europe. However, NAME overestimated the observed concentrations. This was in common with most other models, but was in contrast to other NAME validation studies which had been carried out, indicating either no significant bias or a tendency to underestimate concentrations.

Carruthers et al (1996) focused on the validation of CERC's ADMS model but in the process also assessed the (relative) performance of the R91 model. Model validation was performed against LIDAR data for isolated stacks in flat terrain, across a range of neutral and unstable atmospheric conditions, for receptors between hundreds of metres to 3 kilometres downwind, stack heights ranging from 120 to 260 metres, the inclusion of plume rise and surface roughnesses of 0.2 and 0.5 metres. This study substantiates the conclusions made here that R91 under-predicts σ_y and σ_z. Carruthers et al, 1996 found that for releases with differing site, source and emission characteristics, σ_y estimated from observations was a factor of 1.3 to 1.6 greater than σ_y estimated by R91 and σ_z estimated from observations was a factor of 1.1 to 2.2 greater than σ_z estimated by R91.

Kretzschmar et al (1984) evaluated the ability of a number of Gaussian plume models (including Hosker-Smith, Pasquill, Briggs, Vogt, Klug, SCK, Turner and Doury schemes) to simulate short term emissions at a release height 2 metres above ground level against a tracer experiment performed in a region of flat terrain and agricultural land use. Emissions were constant and started before the sampling in order to allow the plume to reach the receptors at the largest distances downwind. Sampling periods of 30 minutes were assumed. The receptors ranged in distance from the release point (from 0.6 km to 7 km), with the majority between 2 km to 4 km. 56% of the sample periods were in conditions defined as neutral, with 29% in unstable and 15% in stable conditions. However, as the average of the percentage relative difference is presented, the results quoted are largely thought to be independent of atmospheric stability and source-receptor distance. It was found (contrary to Carruthers et al (1996)) that R91 overestimated σ_y (by 20%) relative to measured estimates of σ_y. This may be due to dominance in the contribution from the more distant receptors, as it has been observed in this study that estimates of σ_y in R91 are greater than in NAME at distances greater than 5 km from the release. However, this is not conclusive and due to insufficient information there remains some uncertainty why Kretzschmar et al (1984) observed that R91 overestimated σ_y relative to measured estimates. Direct measurements of the vertical concentration profile were not available and therefore the determination of the vertical dispersion was based on an initial assumption of the shape of the profile, on the principle of mass conservation and on the measurement of the ground level concentration in air. R91 underestimated σ_z (by 23%) relative to measured estimates of σ_z, a result qualitatively and quantitatively analogous to the difference observed between R91 and NAME in this study.

Empirical functions of the dispersion factors, including that used in R91, have been constructed as a function of downwind distance and atmospheric stability. These empirical functions are based on measurements at different locations and, in some cases, different interpolations of the same datasets. Vogt (1977) compared short-term diffusion factors Cu/Q (where C is the air concentration, u is the wind speed and Q is the source term) as a function of distance downwind, x (where y = 0 and z = 0) computed from six sets of curves assuming a 100 m release height and using a single method of determining the atmospheric stability. Vogt found that maxima in Cu/Q generally agreed within a factor of 2 for each set of curves and each stability category considered. However, the downwind location of the maxima differed by as much as an order of magnitude. Vogt’s comparisons were based on one method of determining the stability of the atmosphere, but a variety of methods for classifying atmospheric stability have been proposed by Hanna et al (1977). These different methods have been shown to give significantly different results when applied to the same meteorological data set. To avoid these large differences, the dispersion parameters should be chosen on the basis of as much site-specific information as possible; however, such data is often unavailable, especially when performing assessments in response to an emergency.

Model validation across the range of Gaussian plume models is more readily available but is less indicative of the validity of the approach used in R91 as the values of σ_y and σ_z applied to the Gaussian equation vary widely. Crawford (1978) summarised the likely range of ratio of predicted to observed concentrations for the Gaussian model, indicating that under conditions of flat terrain and steady atmospheric conditions, hourly average concentrations at a specific time and receptor point on the PCL within 10 km of the release point are likely to range from 0.1-10, ie, across two orders of magnitude. Miller and Hively (1987), in a review of validation studies for Gaussian plume atmospheric dispersion models, also detail such ratios of predicted to observed concentrations, applicable to a range of release heights. The review notes that changes in the dispersion factors σ_y and σ_z strongly affect resulting activity concentrations in air calculated by the Gaussian plume model as demonstrated by Pasquill (1974) and Weber (1976).

Evidence detailed above suggests that values of σ_y and σ_z utilised in the R91 Gaussian plume model are, under certain conditions, inappropriate for use, and more specifically at relatively short distances from the release, R91 underestimates the cross-wind and vertical profile of a plume under Pasquill stability category D conditions.

Jones et al (1995) performed a model intercomparison of ADMS and R91. This work demonstrated that, as observed in this study, R91 predicted significantly larger TIACs than the comparative model, in this case ADMS, for all of the distances downwind considered. Analogous to this study, Pasquill stability category D conditions, a roughness length of 0.3 m, and a ground level release were assumed. The assumption of a 30 minute release duration (as opposed to 1 hour assumed in this study) and a source diameter of 1 m (as opposed to a point source) are likely to impact minimally after a few tens of metres and certainly by 1 km. At 1 km and 40 km downwind the relative difference between R91 and ADMS model output varied by approximately a factor of 3.0 and 1.2, respectively, akin to the differences observed in this study between R91 and NAME.

Kretzchmar et al (1983) performed an intercomparison of Gaussian plume models and noted that, for short term releases, ground level activity concentrations in air estimated by R91 were intermediate in terms of the ensemble of twelve combinations (which included Hosker-Smith, Pasquill, Briggs, Vogt, Klug, SCK, Turner and Doury schemes).

NAME has been validated against data from the Kincaid Experiment (Thomson and Jones (2011) and Bowne and Londergan (1983)). The conditions of the model validation were not as considered here. The Kincaid Experiment considered a buoyant plume, a 187 m tall stack, receptors at 0.5 km to 50 km from the stack, a roughness length of 0.1 m, a range of met conditions, not specifically neutral stability and the application of NAME considered the use of puffs as opposed to particles in the modelling of the dispersion. Jones et al (2007) state that the results of this validation exercise compare satisfactorily with observations. The results (Thomson and Jones, 2011) show a small overestimation of the mean concentration with NAME (a fractional bias of -0.025), and the spread in the concentrations predicted by NAME is in good agreement with the observed spread. 74% of values were within a factor of two of the observed concentrations. Despite the disparity between the scenarios considered in the model validation and in this study, the model validation is still demonstrative of the validity of the approach in NAME applied here. Differences between a particle and a puff model run tend to be fairly small. In fact the conditions observed in the Kincaid dataset model validation study are more complex than those considered within this study, therefore strengthening the case for the methods applied in NAME. Of course the model validation is generic to NAME as an entirety and not specific to individual components of the model, such as the cross-wind and vertical spread of the plume and the vertical wind profile.

5 QUALITATIVE ASSESSMENT OF THE DIFFERENCES OBSERVED BETWEEN NAME AND R91 OUTPUT FOR A RANGE OF MODEL RUNS

5.1 Baseline run

This section presents NAME and R91 results obtained if key elements of the baseline run are varied. To provide a context for what follows in this section, the results obtained using the baseline inputs are displayed in Table 9, Figure 8 and Figure 9, which show the time integrated activity concentrations in air (Bq s m^{-3}) as a function of distance downwind on the plume centre line for the baseline runs. Figure 8 and Figure 9 display the same information, but on different vertical axes, so that different degrees of detail can be seen.

The table and figures show that for the baseline run, the R91 results are higher than the NAME results by a factor of between 1.4 and 3.4, and that the two sets of results steadily converge with increasing distance downwind. The results generated in Section 5 should be viewed against the baseline model results. The main factor under consideration will be how the relationship between the NAME and R91 results differs in the following runs compared to what has been observed in the baseline run. In other words, it is the “differences in the differences” between the results which is significant.

As explained in Section 4, differences between the R91 and NAME results for the baseline run can mainly be attributed to corresponding differences in one or more of the parameters σ_y, σ_z and u. Consequently, the variations observed below are considered primarily in the context of these parameters.

Table 9 Ground level time integrated activity concentrations in air (Bq s m^{-3}) as a function of distance downwind for the baseline runs

	1 km	2 km	5 km	10 km	20 km	40 km
NAME baseline model run	$3.8\ 10^{10}$	$1.5\ 10^{10}$	$4.4\ 10^{9}$	$1.8\ 10^{9}$	$7.3\ 10^{8}$	$2.9\ 10^{8}$
R91 baseline model run	$1.3\ 10^{11}$	$4.1\ 10^{10}$	$9.2\ 10^{9}$	$3.1\ 10^{9}$	$1.1\ 10^{9}$	$4.2\ 10^{8}$
(NAME TIAC)/(R91 TIAC)	0.29	0.36	0.48	0.59	0.67	0.70
(R91 TIAC)/(NAME TIAC)	3.4	2.8	2.1	1.7	1.5	1.4

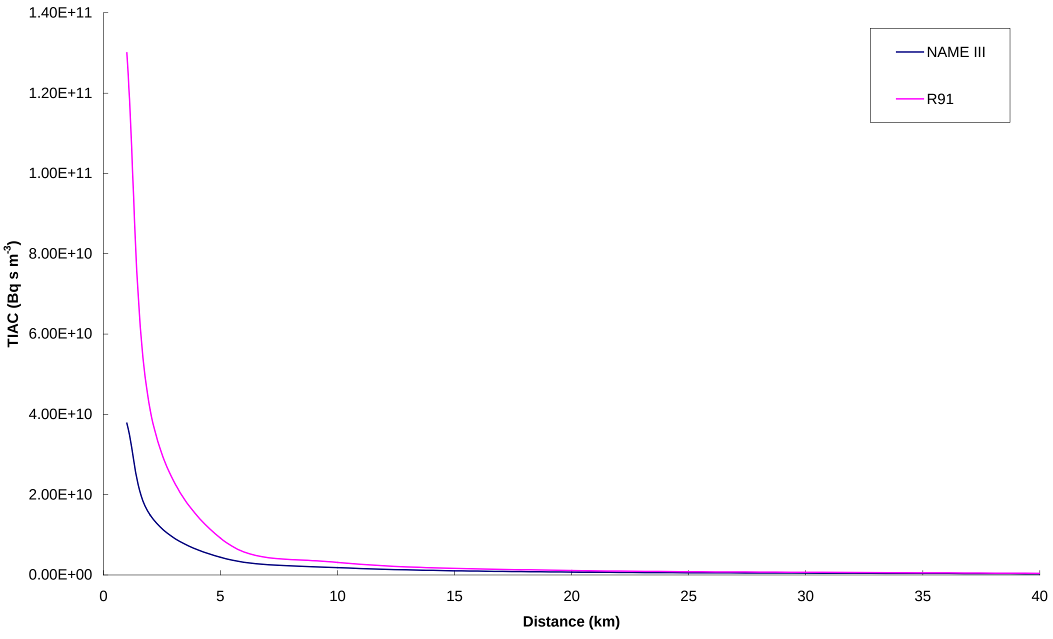

Figure 8 Ground level time integrated activity concentrations in air (Bq s m^{-3}) as a function of distance downwind for the baseline runs

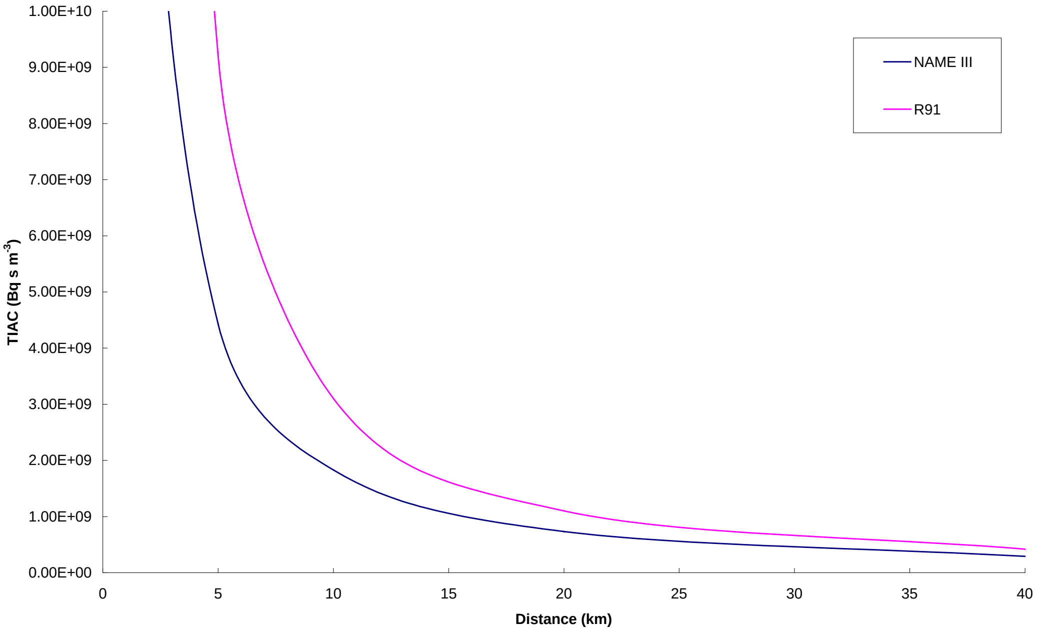

Figure 9 Ground level time integrated activity concentrations in air (Bq s m^{-3}) as a function of distance downwind for the baseline runs (as Figure 8 but using an exaggerated vertical scale)

5.2 Pasquill stability category

Table 10, Figure 10 and Figure 11 all show the time integrated activity concentrations in air (Bq s m^{-3}) as a function of distance downwind for Pasquill stability category A (ie, strongly unstable conditions). Figure 10 and Figure 11 show the same information, but on different vertical axes, so that different degrees of detail can be seen. Similarly, Table 11 and Figure 12 and Figure 13 show the time integrated activity concentrations in air (Bq s m^{-3}) as a function of distance downwind for Pasquill stability category G (strongly stable conditions).

The input parameters used in these runs were identical to those used in Section 5.1, barring modifications to the Pasquill stability category, whereby Category A (surface sensible heat flux: 235 W m^{-2}, mixing layer depth: 1300 m and wind speed: 1 m s^{-1}) and Category G (surface sensible heat flux: -18 W m^{-2}, mixing layer depth: 100 m and wind speed: 1 m s^{-1}) conditions were assumed. Given the low wind speeds considered the NAME model run time was extended to achieve a true time integral of the entire passage of the plume.

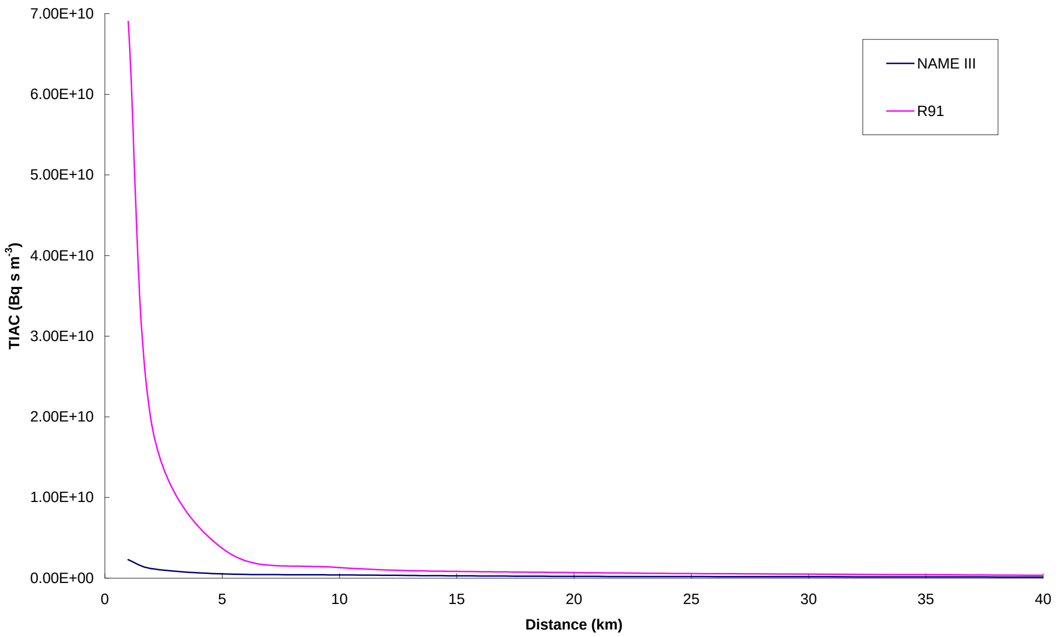

Figure 10 Ground level time integrated activity concentrations in air (Bq s m^{-3}) as a function of distance downwind for Pasquill stability category A

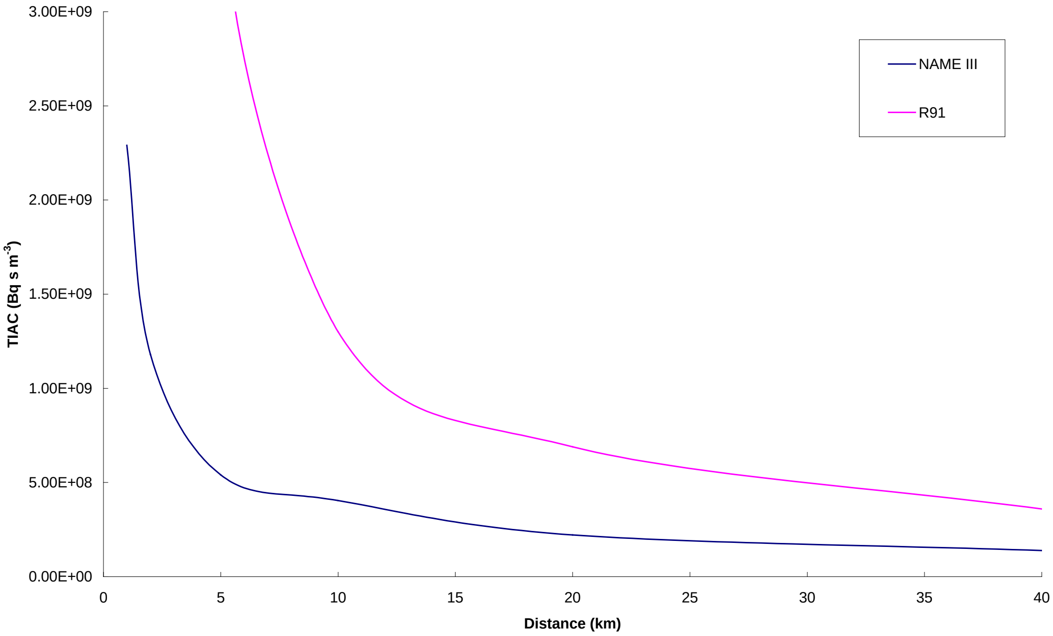

Figure 11 Ground level time integrated activity concentrations in air (Bq s m^{-3}) as a function of distance downwind for Pasquill stability category A

Table 10 Ground level time integrated activity concentrations in air (Bq s m^{-3}) as a function of distance downwind for Pasquill stability category A

	1 km	2 km	5 km	10 km	20 km	40 km
NAME TIAC (Bq s m^{-3})	$2.3\ 10^{9}$	$1.2\ 10^{9}$	$5.4\ 10^{8}$	$4.0\ 10^{8}$	$2.2\ 10^{8}$	$1.4\ 10^{8}$
R91 TIAC (Bq s m^{-3})	$6.9\ 10^{10}$	$1.9\ 10^{10}$	$3.7\ 10^{9}$	$1.3\ 10^{9}$	$6.9\ 10^{8}$	$3.6\ 10^{8}$
(NAME TIAC)/(R91 TIAC)	0.033	0.062	0.15	0.31	0.32	0.39
(R91 TIAC)/(NAME TIAC)	30	16	6.9	3.2	3.1	2.6

Table 11 Ground level time integrated activity concentrations in air (Bq s m^{-3}) as a function of distance downwind for Pasquill stability category G

	1 km	2 km	5 km	10 km	20 km	40 km
NAME TIAC (Bq s m^{-3})	$1.6\ 10^{11}$	$6.0\ 10^{10}$	$1.7\ 10^{10}$	$6.8\ 10^{9}$	$2.7\ 10^{9}$	$1.2\ 10^{9}$
R91 TIAC (Bq s m^{-3})	$1.0\ 10^{12}$	$5.3\ 10^{11}$	$1.5\ 10^{11}$	$5.6\ 10^{10}$	$2.1\ 10^{10}$	$8.3\ 10^{9}$
(NAME TIAC)/(R91 TIAC)	0.16	0.11	0.12	0.12	0.13	0.14
(R91 TIAC)/(NAME TIAC)	6.3	8.8	8.7	8.2	7.7	7.2

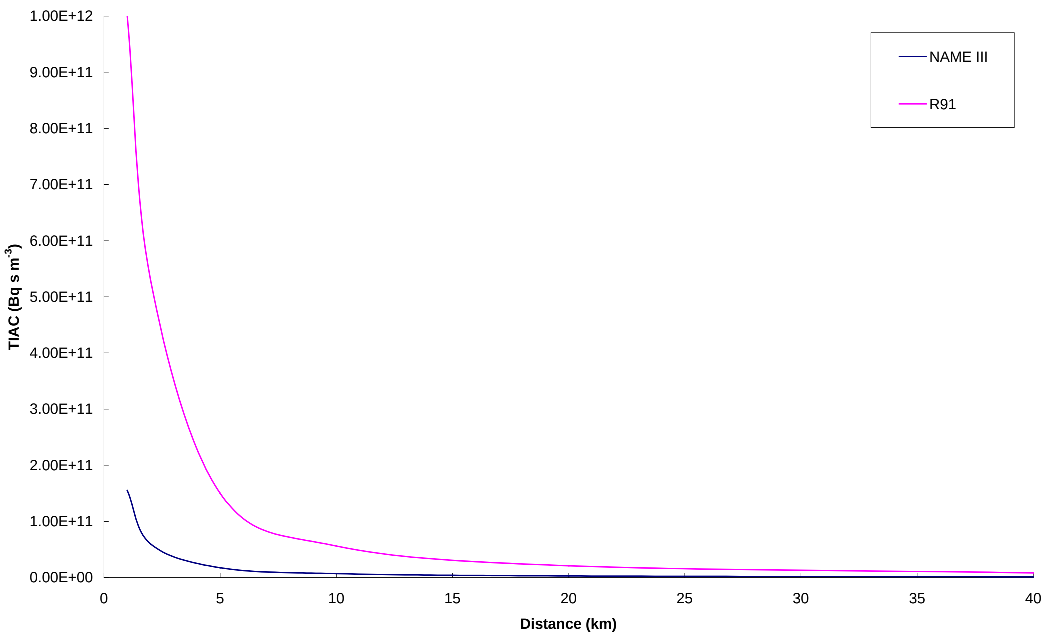

Figure 12 Ground level time integrated activity concentrations in air (Bq s m^{-3}) as a function of distance downwind for Pasquill stability category G

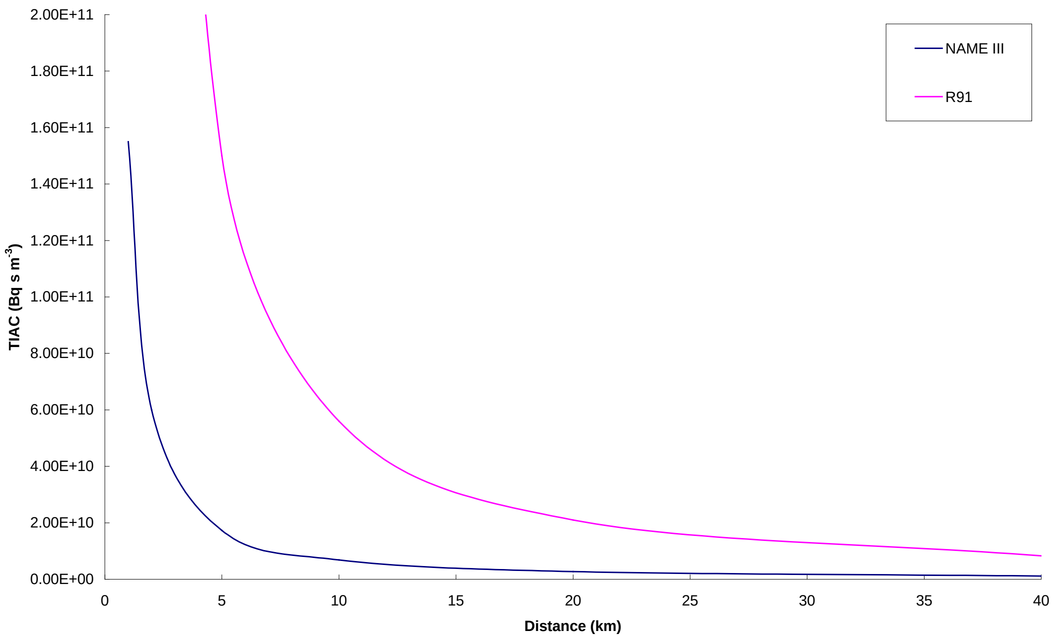

Figure 13 Ground level time integrated activity concentrations in air (Bq s m^{-3}) as a function of distance downwind for Pasquill stability category G

Time integrated activity concentrations in air estimated using R91 are greater than for NAME at all distances downwind (considered in this study) for Pasquill stability category A and category G conditions, as observed for baseline Pasquill stability category D conditions. A further resemblance to the baseline model run is the trend for model estimates under category A and G conditions to converge at large distances from the release; however, this is where the similarities end.

For a release in Pasquill stability category A conditions the two curves (in Figure 10 and Figure 11) are more divergent at relatively small distances downwind than for category D and G conditions. The two curves converge relatively quickly, and so are less divergent than under category G conditions at larger distances (but still more divergent than under category D conditions). More specifically, the ratio of R91/NAME at 1 km is 30 and at 40 km is 2.6. In comparison the ratios for the baseline run are 3.4 at 1 km and 1.4 at 40 km. Hence, the NAME and R91 results were found to be more similar for neutral atmospheric conditions than for unstable conditions.

The reason for a greater disparity between NAME and R91 model output in unstable conditions is likely to lie with the different methods of describing turbulence and therefore the effective differences between σ_y and σ_z applied by R91 and the respective approach in NAME used to describe the cross-wind and vertical spread of the plume (detailed in Sections 4.1 and 4.2, respectively). However, the difference in the methods describing the advection of the plume may also be a contributory factor, especially for relatively low wind speeds where R91 does not account for upwind and along-wind spread of the plume (see Section 5.4 for details).

For Pasquill stability category A conditions, relatively large σ_y and σ_z would be expected as a result of greater horizontal and vertical mixing due to significant levels of thermally driven turbulence and greater instability. It is apparent from Table 9 and Table 10 that at a few kilometres downwind from the release there is a significant decrease in NAME predicted time integrated activity concentrations in air for category A conditions and therefore presumably a significant increase in the cross-wind and/or vertical spread of the plume. Without further investigation it is difficult to differentiate between vertical and cross-wind components to identify the contribution from individual factors. However, evidence suggests that the disparity in the models' description of the vertical spread of the plume is a factor. As a plume is advected downwind it spreads vertically within the boundary layer. Once the plume described by NAME (which spreads at a faster rate) is capped by the top of the boundary layer, further dispersion in the vertical plane is restricted in NAME and the concentrations estimated by both models begin to converge (at distances greater than 1 km from the release), as demonstrated by Table 10.

For a release in Pasquill stability category G conditions, the two curves (see Figure 12 and Figure 13) are more divergent at all distances downwind than for the baseline run (but more especially at relatively large distances). Apart from the ratio at 1 km being 6.3, the two curves do slowly converge with increasing distance (the ratio of R91/NAME at 2 km is 8.8 and at 40 km is 7.2). The ratios for the baseline runs are 3.4 at 1 km and 1.4 at 40 km. Hence, the NAME and R91 results were found to be more similar for neutral atmospheric conditions than for stable conditions.

For Pasquill stability category G conditions, a relatively small σ_z would be expected as a result of less vertical mixing due to minimal mechanically and thermally driven turbulence (buoyancy effects would act to suppress turbulence in stable conditions). Despite limited horizontal mixing due to minimal mechanically and thermally driven turbulence a relatively large value of σ_y would be expected due to an increase in wind meander (and in fact R91 assumes σ_y is greater in Pasquill stability category G conditions than in category D conditions). It is reasonable to assume that meander is the dominant factor when determining the crosswind spread of the plume in category G conditions. The crosswind spread is described by 0.17 x (where ‘x’ is the distance downwind) in R91 (applying Equation 2) and in NAME by 0.5 t (where ‘t’ is the time since the release) which approximates to 0.5 x for a wind speed of 1 m s^{-1} (although it ceases to increase linearly beyond about one hour’s travel time). Hence the crosswind spread in NAME is approximately three times greater than in R91.

For a release in Pasquill stability category G conditions, the contrast in concentrations, notably in R91, is starker for changes in light winds compared to changes in strong winds (as a result of the reciprocal relationship between air concentration and wind speed). Furthermore, in stable conditions, u can change significantly (in relative terms) with height (akin to an almost linear profile near the ground) and so the difference in approach between NAME (using a wind profile to describe particle advection) and R91 (using a single wind speed at a height of 10 m to describe particle advection) could be significant. In addition at relatively low wind speeds R91 does not account for upwind and along-wind spread of the plume (see Section 5.4 for details). It is apparent from Table 9 and Table 11 that at all distances downwind considered in this study, but most notably at relatively large distances, there exists a much larger increase in the R91 predicted TIACs for Pasquill stability category G conditions (compared to baseline Pasquill stability category D conditions). The reason for the greater disparity between NAME and R91 model output for Pasquill stability category G conditions is the difference in the methods used to describe the crosswind spread of the plume, vertical spread of the plume and the wind profile. However, without further investigation it is difficult to differentiate between the components and identify the contribution from individual factors.

Pasquill stability categories are in a sense unbounded and categories A and G are no exception. Within Pasquill stability categories A and G stability can become arbitrarily unstable or stable, respectively, and therefore there exists the potential for a large range of results. Within a single stability category (all other conditions being the same) NAME will estimate varying plume widths and varying upwind spread, whereas R91 will always estimate the same plume width. This is due to the large range in values of heat flux applicable to a single stability category.

5.3 Release height

Table 12 and Figure 14 show the time integrated activity concentration in air (Bq s m^{-3}) as a function of distance downwind for a release height of 200 m.

Input parameters were identical to those used in Section 5.1, barring modifications to the release height, whereby a height of 200 m was assumed.

Table 12 Ground level time integrated activity concentrations in air (Bq s m^{-3}) as a function of distance downwind for release height of 200 m

	1 km	2 km	5 km	10 km	20 km	40 km
NAME TIAC (Bq s m^{-3})	1.5 10^9	3.1 10^9	2.5 10^9	1.4 10^9	6.3 10^8	2.9 10^8
R91 TIAC (Bq s m^{-3})	9.8 10^6	1.4 10^9	3.5 10^9	2.0 10^9	9.0 10^8	3.8 10^8
(NAME TIAC)/(R91 TIAC)	150	2.2	0.72	0.71	0.70	0.76
(R91 TIAC)/(NAME TIAC)	0.0066	0.45	1.4	1.4	1.4	1.3

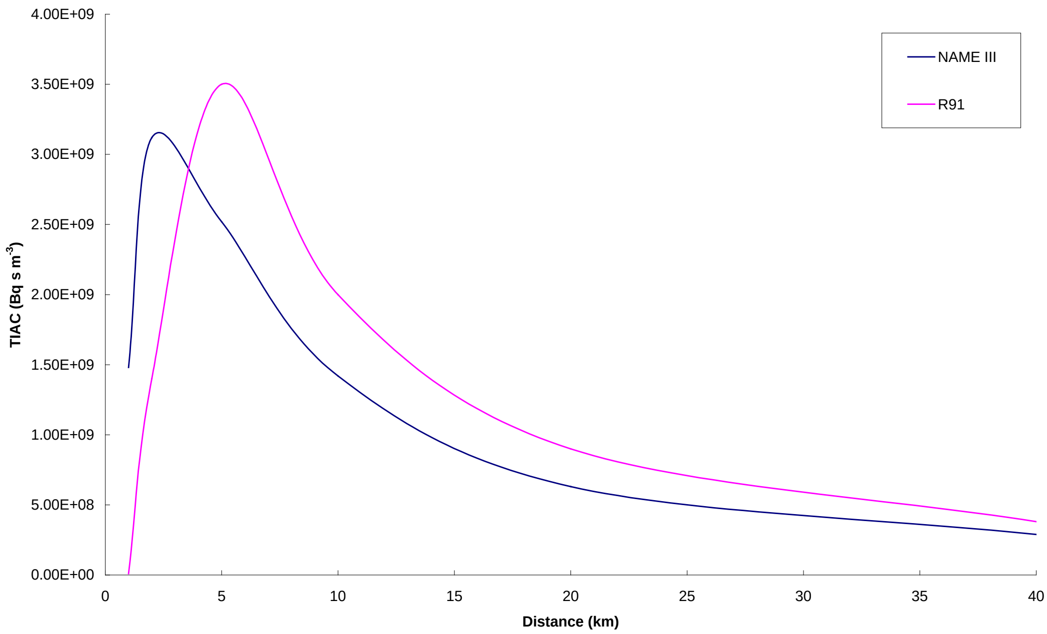

Figure 14 Ground level time integrated activity concentrations in air (Bq s m^{-3}) as a function of distance downwind for a release height of 200 m

Both sets of values initially increase with increasing distance (Figure 14), which is to be expected for an elevated release because the plume travels a significant distance downwind before the main body of the plume mixes down to the ground.

Table 12 and Figure 14 show that, for an increase in release height, and relatively short distances downwind (notably 1 km), NAME gives a result which is more than two orders of magnitude greater than R91. However, at increasingly large release heights, the TIACs associated with the extreme tail of the plume impinging on the ground at relatively short distances downwind are very sensitive, for example to changes in model input parameters. It has been explained in Section 4.2 that for distances downwind of less than about 20 km, values of σ_z estimated by R91 are smaller than for NAME. This corresponds to less vertical mixing. A consequence of this is that the R91 plume takes longer (or, more specifically, a greater distance downwind) to reach ground level. This is thought likely to account for the relationship shown in Figure 14. The same reasoning applies when explaining why the peak in the activity concentration in air in NAME resides closer to the release than in R91. Presumably this effect dominates over the higher effective advection speed in NAME which would act to increase the downwind distance at which the plume grounds (at least for Pasquill Stability D conditions). However, this does not explain why the NAME peak is lower than the later R91 peak. The likely explanation for this is a greater value of σ_y for NAME (as identified in Section 4.1) implying a greater spread of the plume in the horizontal direction over a shorter downwind distance than the R91 plume. Table 13 and Figure 15 consider a more comprehensive number of focused data points (1, 2, 2.5, 3, 4, 5 and 10 km downwind; no data were available for R91 at 2.5 km downwind) and confirm that the NAME peak is genuinely lower than the later R91 peak.

The two sets of results in Figure 14 cross over at approximately 4 km downwind, subsequently diverge to approximately 7 km, with R91 estimates of time integrated activity concentrations in air greater than those estimated by NAME, and thereafter slowly converge. This pattern, after about 7 km, is similar to that observed for the baseline model run assuming a 10 m release height.

It should also be noted that Figure 16 in Clarke (1979) shows the curve for a 200 m release height as being undefined for distances less than about 2 km, and so the R91 value above for 1 km should be treated with caution.

Table 13 Ground level time integrated activity concentrations in air (Bq s m^{-3}) as a function of distance downwind for release height of 200 m

	1 km	2 km	2.5 km	3 km	4 km	5 km	10 km
NAME TIAC (Bq s m^{-3})	1.5 10^9	3.1 10^9	3.3 10^9	3.2 10^9	2.9 10^9	2.5 10^9	1.4 10^9
R91 TIAC (Bq s m^{-3})	9.8 10^6	1.4 10^9	N/A	3.1 10^9	3.6 10^9	3.5 10^9	2.0 10^9
(NAME TIAC)/(R91 TIAC)	150	2.2	N/A	1.0	0.79	0.72	0.71
(R91 TIAC)/(NAME TIAC)	0.0066	0.45	N/A	0.98	1.3	1.4	1.4

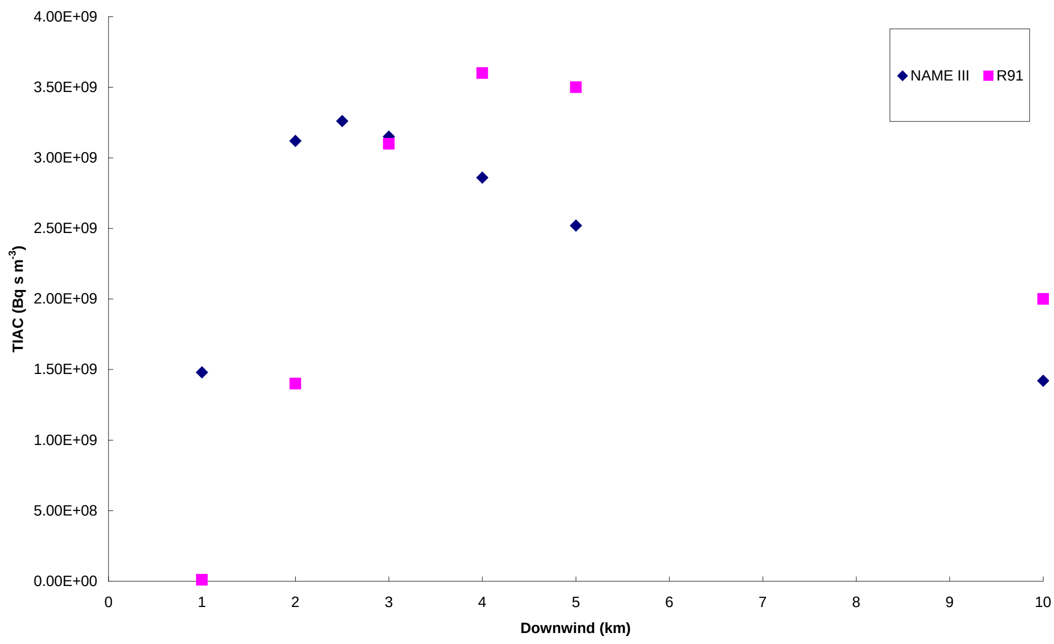

Figure 15 Ground level time integrated activity concentrations in air (Bq s m^{-3}) as a function of distance downwind for a release height of 200 m

There is evidently a large difference between estimated time integrated activity concentrations in air for releases at 10 m (Table 9) and 200 m (Table 12) above ground level. For a release at 80 m above ground level NAME estimates time integrated activity concentrations in air within a factor of 1.5 of the baseline (10 m release height) model output, for all distances downwind considered in this study. The same affinity between 10 m and 80 m release height model estimates applies to the R91 method and respective model output. Note that, for the purposes of brevity, detailed model estimates of time integrated activity concentrations in air for a release at 80 m above ground level are not included here.

5.4 Low wind speeds

Table 14 and Table 15 show the time integrated activity concentration in air (Bq s m^{-3}) as a function of distance downwind for Pasquill stability category A, and for different wind speeds. Similarly, Table 16 and Table 17 show the time integrated activity concentration in air (Bq s m^{-3}) as a function of distance downwind for Pasquill stability category G, for different wind speeds. Input parameters were identical to those used in Section 5.2, barring modifications to the wind speed.

It should be noted that because of large NAME model run times for runs at low wind speeds over a relatively large domain, some of the following runs did not attempt to generate results beyond 5 km downwind. These are termed “short range” runs.

Table 14 Ratios of R91 and NAME ground level time integrated activity concentrations in air (Bq s m^{-3}) as a function of distance downwind and wind speed for Pasquill stability category A (long range runs)

	1 km	2 km	5 km	10 km	20 km	40 km
NAME TIAC (Bq s m^{-3}) for wind speed of 1.0 m s^{-1}	2.3 10^{9}	1.2 10^{9}	5.4 10^{8}	4.0 10^{8}	2.2 10^{8}	1.4 10^{8}
R91 TIAC (Bq s m^{-3}) for wind speed of 1.0 m s^{-1}	6.9 10^{10}	1.9 10^{10}	3.7 10^{9}	1.3 10^{9}	6.9 10^{8}	3.6 10^{8}
NAME TIAC (Bq s m^{-3}) for wind speed of 0.5 m s^{-1}	2.2 10^{9}	1.2 10^{9}	6.1 10^{8}	4.3 10^{8}	2.7 10^{8}	1.1 10^{8}
R91 TIAC (Bq s m^{-3}) for wind speed of 0.5 m s^{-1}	1.1 10^{11}	3.1 10^{10}	6.4 10^{9}	N/A	N/A	N/A
(R91 TIAC)/(NAME TIAC) for wind speed of 1.0 m s^{-1}	30	16	6.9	3.2	3.1	2.6
(R91 TIAC)/(NAME TIAC) for wind speed of 0.5 m s^{-1}	51	26	12	N/A	N/A	N/A

Table 15 Ratios of R91 and NAME ground level time integrated activity concentrations in air (Bq s m^{-3}) as a function of distance downwind and wind speed for Pasquill stability category A (short range runs)

	1 km	2 km	5 km
NAME TIAC (Bq s m^{-3}) for wind speed of 0.8 m s^{-1}	2.3 10^{9}	1.1 10^{9}	4.9 10^{8}
R91 TIAC (Bq s m^{-3}) for wind speed of 0.8 m s^{-1}	7.9 10^{10}	2.2 10^{10}	4.6 10^{9}
NAME TIAC (Bq s m^{-3}) for wind speed of 0.1 m s^{-1}	1.9 10^{9}	1.2 10^{9}	6.0 10^{8}
R91 TIAC (Bq s m^{-3}) for wind speed of 0.1 m s^{-1}	3.0 10^{11}	8.3 10^{10}	1.7 10^{10}
(R91 TIAC)/(NAME TIAC) for wind speed of 0.8 m s^{-1}	34	20	9.4
(R91 TIAC)/(NAME TIAC) for wind speed of 0.1 m s^{-1}	160	70	28

Table 16 Ratios of R91 and NAME ground level time integrated activity concentrations in air (Bq s m^{-3}) as a function of distance downwind and wind speed for Pasquill stability category G (long range runs)

	1 km	2 km	5 km	10 km	20 km	40 km
NAME TIAC (Bq s m^{-3}) for wind speed of 1.0 m s^{-1}	1.6 10^{11}	6.0 10^{10}	1.7 10^{10}	6.8 10^{9}	2.7 10^{9}	1.2 10^{9}
R91 TIAC (Bq s m^{-3}) for wind speed of 1.0 m s^{-1}	1.0 10^{12}	5.3 10^{11}	1.5 10^{11}	5.6 10^{10}	2.1 10^{10}	8.3 10^{9}
NAME TIAC (Bq s m^{-3}) for wind speed of 0.5 m s^{-1}	1.2 10^{11}	4.6 10^{10}	1.4 10^{10}	5.7 10^{9}	2.3 10^{9}	1.0 10^{9}
R91 TIAC (Bq s m^{-3}) for wind speed of 0.5 m s^{-1}	1.5 10^{12}	7.6 10^{11}	2.2 10^{11}	N/A	N/A	N/A
(R91 TIAC)/(NAME TIAC) for wind speed of 1.0 m s^{-1}	6.5	8.8	8.7	8.2	7.7	7.2
(R91 TIAC)/(NAME TIAC) for wind speed of 0.5 m s^{-1}	12	16	17	N/A	N/A	N/A

Table 17 Ratios of R91 and NAME ground level time integrated activity concentrations in air (Bq s m^{-3}) as a function of distance downwind and wind speed for Pasquill stability category G (short range runs)

	1 km	2 km	5 km
NAME TIAC (Bq s m^{-3}) for wind speed of 0.8 m s^{-1}	1.4 10^{11}	5.5 10^{10}	1.6 10^{10}
R91 TIAC (Bq s m^{-3}) for wind speed of 0.8 m s^{-1}	1.2 10^{12}	6.0 10^{11}	1.8 10^{11}
NAME TIAC (Bq s m^{-3}) for wind speed of 0.1 m s^{-1}	7.6 10^{10}	3.0 10^{10}	8.6 10^{9}
R91 TIAC (Bq s m^{-3}) for wind speed of 0.1 m s^{-1}	3.3 10^{12}	1.7 10^{12}	5.0 10^{11}
(R91 TIAC)/(NAME TIAC) for wind speed of 0.8 m s^{-1}	8.5	11	11
(R91 TIAC)/(NAME TIAC) for wind speed of 0.1 m s^{-1}	43	56	58

Gaussian plume models are recognised to model dispersion in calm conditions poorly (see ADMLC (1997) and Thomson and Manning (2001)). R91 cannot be used when the wind speed is zero, as the basic equation includes the reciprocal of the wind speed. However, the model is also inappropriate at low but non-zero wind speeds, as the assumptions on which it is based no longer adequately represent the physical processes involved. In particular, the model assumes that dispersion along the wind direction is small compared to advection by the mean wind. This assumption is not correct at low wind speeds in both unstable atmospheric conditions, where turbulent processes are likely to be dominant, and stable conditions, where meander processes are likely to be dominant. In addition, R91 is unable to model upwind spread in light wind conditions (ADMLC, 1999). R91's inability to model dispersion in calm conditions is illustrated by the results detailed in Table 14 to Table 17, which show that the difference between the results for R91 and NAME increase as wind speed decreases. The above results do not indicate a "threshold" as such, but indicate a continuing divergence in the R91 and NAME results with decreasing wind speed.

Irrespective of the stability conditions, R91 consistently estimates larger time integrated activity concentrations in air than NAME. Under Pasquill stability category A conditions R91 estimates increase significantly as wind speeds decrease, however NAME estimates vary negligibly. The trend is for the endpoints to converge with increasing distance from the release. One unexpected observation is that for category G conditions the R91 and NAME results appear to diverge with increased distance downwind. This is the opposite of what has been found in most of the other runs. However, the results are already so divergent at that point that it may be unwise to speculate on the exact reason for this, particularly as there are only limited data to consider. Furthermore the TIACs estimated by R91 increase as wind speed decreases but conversely the NAME activity concentrations in air decrease as the wind speed decreases under category G conditions (thought to be a result of the greater degree of upwind spread for smaller wind speeds in NAME).

The most likely cause of the additional differences observed in this section over those for the baseline run are a result of u. σ_y is also a factor because the wind direction fluctuation term assumed in R91 is a function of wind speed; however, the contribution from this term is determined by the square root of the reciprocal of u which is less significant than the contribution from the advection term which is purely the reciprocal of u.

5.5 High wind speeds

Table 18 and Table 19 show the time integrated activity concentration in air (Bq s m^{-3}) as a function of distance downwind for higher wind speeds of 10 m s^{-1} and 15 m s^{-1}. Similarly, Figure 16 and Figure 17 show the same information, but on different vertical axes, so that different degrees of detail can be seen. Input parameters were identical to those used in Section 5.1 (assuming neutral stability), barring modifications to the wind speed, whereby speeds of 10 m s^{-1} and 15 m s^{-1} were assumed.

Table 18 Ground level time integrated activity concentrations in air (Bq s m^{-3}) as a function of distance downwind for wind speed of 10 m s^{-1}

	1 km	2 km	5 km	10 km	20 km	40 km
NAME TIAC (Bq s m^{-3})	2.2 10^{10}	9.0 10^{9}	2.8 10^{9}	1.2 10^{9}	5.2 10^{8}	2.2 10^{8}
R91 TIAC (Bq s m^{-3})	8.0 10^{10}	2.5 10^{10}	5.7 10^{9}	2.0 10^{9}	7.0 10^{8}	2.6 10^{8}
(NAME TIAC)/(R91TIAC)	0.28	0.36	0.50	0.61	0.75	0.85
(R91TIAC)/(NAME TIAC)	3.6	2.8	2.0	1.7	1.3	1.2

Table 19 Ground level time integrated activity concentrations in air (Bq s m^{-3}) as a function of distance downwind for wind speed of 15 m s^{-1}

	1 km	2 km	5 km	10 km	20 km	40 km
NAME TIAC (Bq s m^{-3})	1.5 10^{10}	6.0 10^{9}	2.0 10^{9}	8.4 10^{8}	4.3 10^{8}	1.8 10^{8}
R91 TIAC (Bq s m^{-3})	5.7 10^{10}	1.8 10^{10}	4.1 10^{9}	1.4 10^{9}	5.1 10^{8}	1.9 10^{8}
(NAME TIAC)/(R91 TIAC)	0.27	0.34	0.48	0.60	0.85	0.92
(R91 TIAC)/(NAME TIAC)	3.7	3.0	2.1	1.7	1.2	1.1

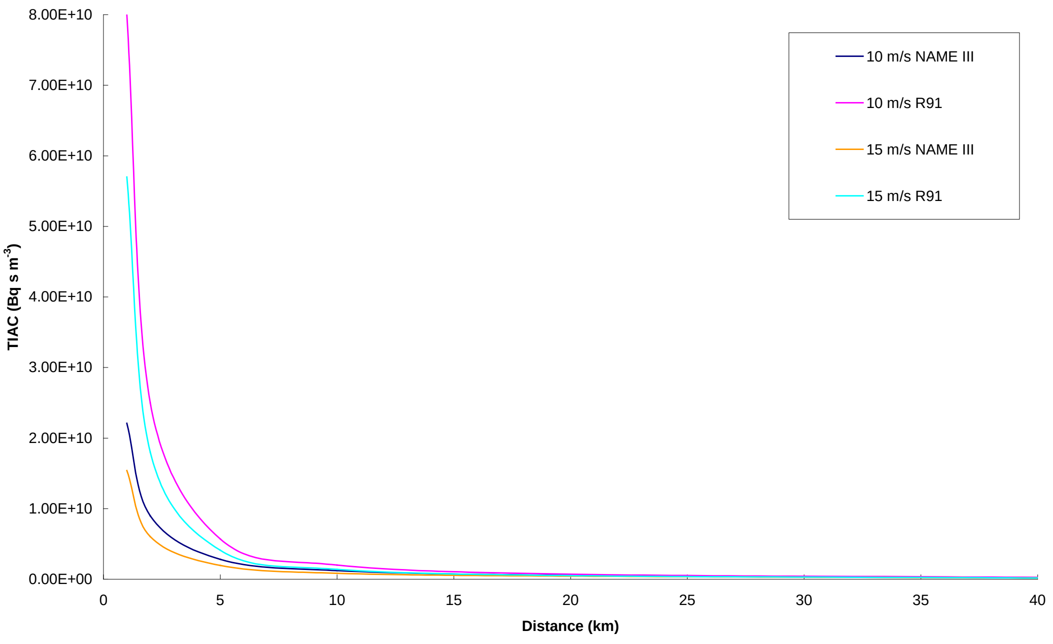

Figure 16 Ground level time integrated activity concentrations in air (Bq s m^{-3}) as a function of distance downwind for wind speeds of 10 m s^{-1} and 15 m s^{-1}

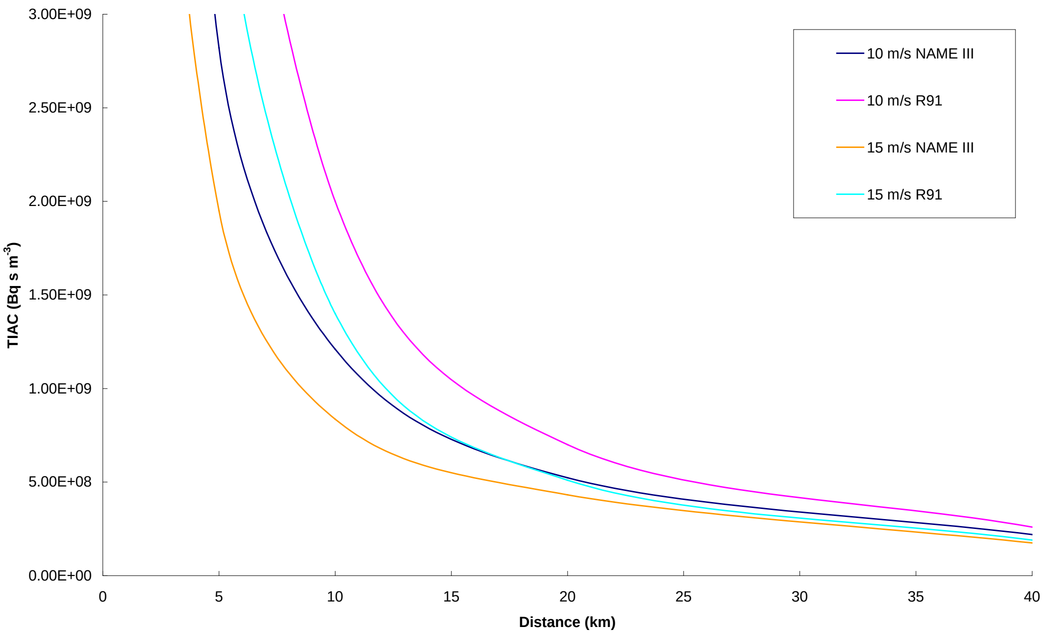

Figure 17 Ground level time integrated activity concentrations in air (Bq s m^{-3}) as a function of distance downwind for wind speeds of 10 m s^{-1} and 15 m s^{-1}

In all cases, for a single wind speed, R91 estimates of the time integrated activity concentration in air are greater than the respective estimates in NAME. The results converge with increasing distance downwind and are very similar at 40 km. At short distances downwind, the R91 TIACs for 10 m s^{-1} and 15 m s^{-1} wind speeds are higher than the corresponding NAME TIACs. At larger distances downwind (20 km or greater), TIACs for a wind speed of 10 m s^{-1} are higher than the TIACs for a wind speed of 15 m s^{-1}, irrespective of the model considered in this study. Or, to put it another way, at short distances downwind the curves are “paired” according to the model used whereas at large distances downwind they appear to be “paired” according to wind speed.

The differences between the results of R91 and NAME runs for a wind speed of 10 m s^{-1} are analogous to the differences for the R91 and NAME baseline runs. The baseline runs show slightly better agreement at smaller distances downwind (at 1 km there is a ratio of 3.4 compared to a ratio of 3.6 for the 10 m s^{-1} runs), but the 10 m s^{-1} runs show a marginally better agreement at greater distances downwind (at 40 km there is a ratio of 1.2 compared to a ratio of 1.4 for the baseline runs). The ratios for the 15 m s^{-1} runs are very similar to those for the 10 m s^{-1} runs (3.7 at 1 km and 1.1 at 40 km).

As the only variation of the parameters from those used in the baseline runs is wind speed, any additional differences observed between the curves can be attributed to u and/or σ_y which is a function of u. The relatively large wind speeds assumed in this scenario imply σ_{yw} will be relatively small and σ_{yt}, which is not a function of u, will dominate the contribution to σ_y.

There are indications that where mechanical turbulence is the dominant form of turbulence, for example in Pasquill stability D conditions associated with high wind speeds, R91 and NAME appear to be in relatively good agreement.

5.6 Release duration

Table 20, Figure 18 and Figure 19 show the time integrated activity concentration in air (Bq s m^{-3}) as a function of distance downwind for varying release durations, with the figures showing the same information, but on different vertical axes, so that different degrees of detail can be seen. Input parameters were identical to those used in Section 5.1, barring modifications to the release duration, where durations of 4, 8 and 12 hours were assumed (but the magnitude of the release kept the same). These were compared with the results obtained from the baseline runs. The time integrated activity concentrations in air in this scenario were not all estimated at the same time after the release but were estimated at a time specific to the release duration, when the entire release was deemed to have passed all of the receptors concerned (ie, the total time-integrated activity for the release event).

Table 20 Ground level time integrated activity concentrations in air (Bq s m^{-3}) as a function of distance downwind and release duration

	1 km	2 km	5 km	10 km	20 km	40 km
NAME -1 hour release duration	$3.8\ 10^{10}$	$1.5\ 10^{10}$	$4.4\ 10^{9}$	$1.8\ 10^{9}$	$7.3\ 10^{8}$	$2.9\ 10^{8}$
NAME - 4 hour release duration	$3.8\ 10^{10}$	$1.5\ 10^{10}$	$4.4\ 10^{9}$	$1.8\ 10^{9}$	$7.7\ 10^{8}$	$3.0\ 10^{8}$
NAME - 8 hour release duration	$3.8\ 10^{10}$	$1.5\ 10^{10}$	$4.5\ 10^{9}$	$1.9\ 10^{9}$	$7.5\ 10^{8}$	$3.0\ 10^{8}$
NAME - 12 hour release duration	$3.9\ 10^{10}$	$1.5\ 10^{10}$	$4.6\ 10^{9}$	$1.8\ 10^{9}$	$7.5\ 10^{8}$	$2.9\ 10^{8}$
R91 - 1 hour release duration	$1.3\ 10^{11}$	$4.1\ 10^{10}$	$9.2\ 10^{9}$	$3.1\ 10^{9}$	$1.1\ 10^{9}$	$4.2\ 10^{8}$
R91 - 4 hour release duration	$8.1\ 10^{10}$	$2.5\ 10^{10}$	$5.8\ 10^{9}$	$1.9\ 10^{9}$	$7.0\ 10^{8}$	$2.6\ 10^{8}$
R91 - 8 hour release duration	$6.4\ 10^{10}$	$2.0\ 10^{10}$	$4.6\ 10^{9}$	$1.6\ 10^{9}$	$5.6\ 10^{8}$	$2.1\ 10^{8}$
R91 - 12 hour release duration	$4.8\ 10^{10}$	$1.5\ 10^{10}$	$3.5\ 10^{9}$	$1.2\ 10^{9}$	$4.2\ 10^{8}$	$1.6\ 10^{8}$

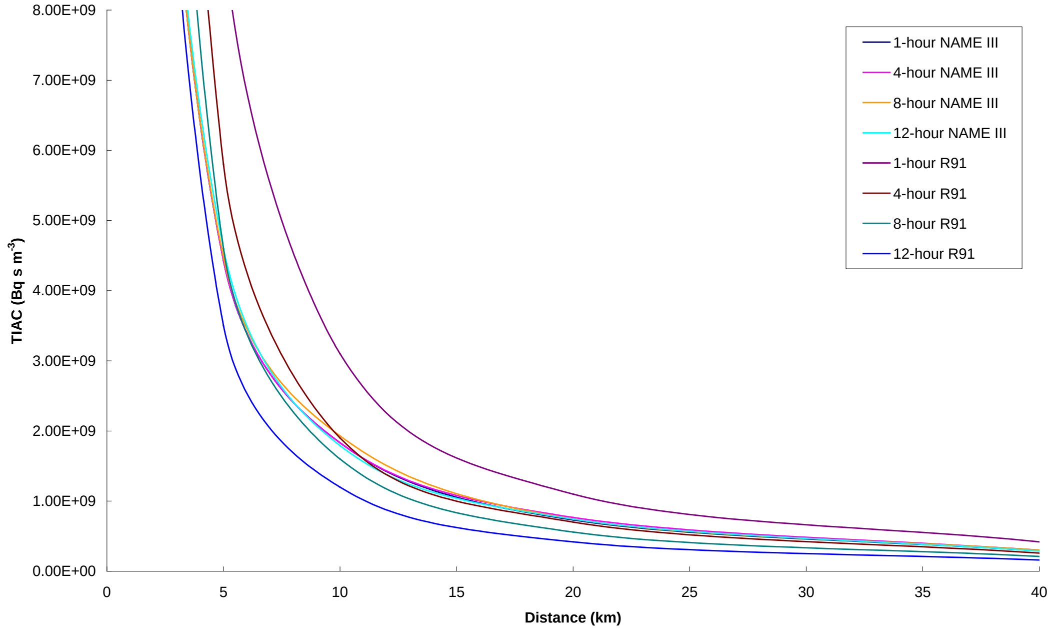

Figure 18 Ground level time integrated activity concentrations in air (Bq s m^{-3}) as a function of distance downwind and release duration

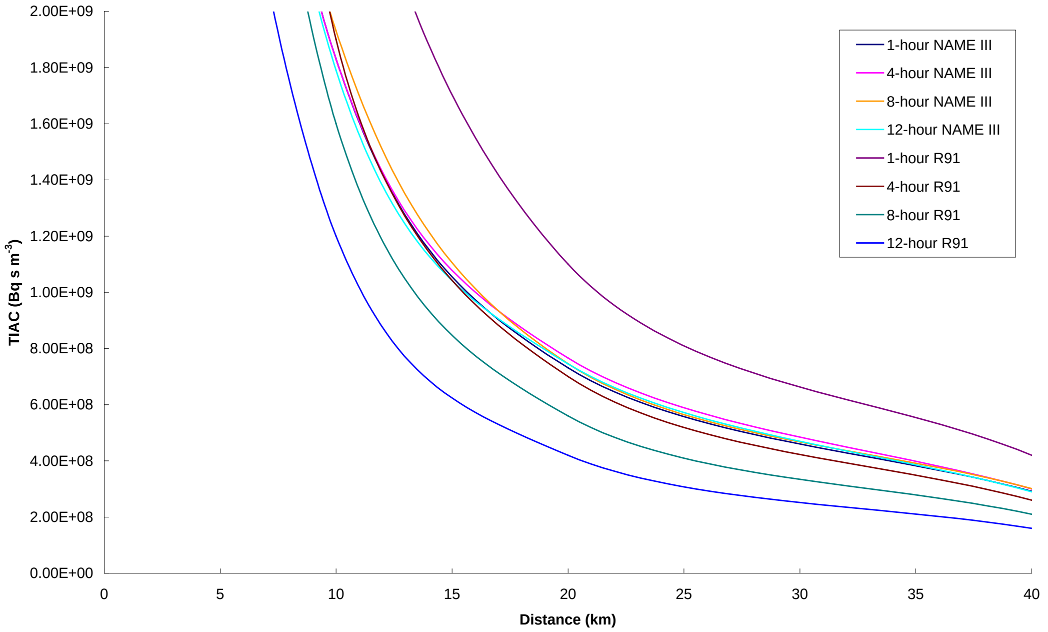

Figure 19 Ground level time integrated activity concentrations in air (Bq s m^{-3}) as a function of distance downwind and release duration

At 1 km downwind from the release, all NAME estimated time integrated activity concentrations in air are less than R91 concentrations, irrespective of the release duration, however this is the only distance (of those considered in this study) where this is the case. At 5km downwind and greater, NAME estimated TIACs for relatively large release durations are greater than the respective R91 estimated TIACs.

Table 20, Figure 18 and Figure 19 show that the four sets of NAME results are very similar for releases of 1, 4, 8 and 12 hours (the 4 sets of results lie almost along a single line in Figure 18 and Figure 19), ie, NAME estimated TIACs are not a function of release duration. This is because fluctuations in wind direction over time periods of the order of hours are represented explicitly through time dependent input meteorology rather than through a statistical parameterization. In contrast, as release duration increases when modelled by R91, the concentrations estimated by R91 decrease. At short distances downwind, the NAME results are closest to the longest-release R91 results. Conversely, at larger distances downwind, the NAME results become close to the shortest-release R91 results. This reflects a limitation in the use of NAME with fixed met data over a release period of the order of hours. NAME would account for changes in the large-scale wind direction explicitly through its meteorological data inputs if "real" meteorological data were used. It is possible, but not recommended, to modify the meander term in NAME explicitly within the input interface.

It is relevant that in R91, σ_{yw} (and consequently σ_y) is a function of release duration. As release duration increases, σ_{yw} increases. Hence, there is a decrease in activity concentration in air if there is an increase in release duration. This means that the relationships between the R91 derived curves in Figure 18 and Figure 19 can be explained by considering the effect of an increase in the release duration in equation 12 in Clarke (1979) (see Equation 2).

Given this fundamental difference, the improved agreement between R91 and NAME at larger release durations, notably 4 and 8 hours, is thought to be due to deficiencies and differences in modelling approaches cancelling each other out rather than the models both successfully describing the conditions being modelled. From a positive perspective this is an indication of the robustness of R91 over such release durations.

5.7 Offset in the wind direction

Table 21 and Table 22 show the time integrated activity concentrations in air (Bq s m^{-3}) as a function of distance downwind for offsets in the true wind direction, to investigate the influence of an error in the predicted wind direction. Input parameters were identical to those used in Section 5.1, barring modifications to the wind direction, whereby directions 10 degrees and 20 degrees off axis were assumed. These results were compared with the results obtained from the baseline runs. Note that the time integrated activity concentrations in air in Table 22 at 20 km and 40 km were not available in NAME because these points were located in the extreme tail of the plume and reliable estimates could not be given due to the statistical noise inherent in such an approach.

Table 21 Ground level time integrated activity concentrations in air (Bq s m^{-3}) as a function of distance downwind at 10 degrees off the axis of the plume centre line

	1 km	2 km	5 km	10 km	20 km	40 km
NAME	$2.1\ 10^{10}$	$6.9\ 10^{9}$	$1.4\ 10^{9}$	$3.7\ 10^{8}$	$7.0\ 10^{7}$	$1.1\ 10^{7}$
R91	$3.3\ 10^{10}$	$9.2\ 10^{9}$	$1.9\ 10^{9}$	$6.0\ 10^{8}$	$2.0\ 10^{8}$	$7.0\ 10^{7}$

Table 22 Ground level time integrated activity concentrations in air (Bq s m^{-3}) as a function of distance downwind at 20 degrees off the axis of the plume centre line

	1 km	2 km	5 km	10 km	20 km	40 km
NAME	$3.1\ 10^{9}$	$5.8\ 10^{8}$	$2.8\ 10^{7}$	$2.4\ 10^{6}$	N/A	N/A
R91	$3.2\ 10^{8}$	$8.9\ 10^{7}$	$1.5\ 10^{7}$	$3.3\ 10^{6}$	$7.0\ 10^{5}$	$1.8\ 10^{5}$

It is evident from Section 4.1 that at 2 km or less downwind (for the baseline model run and those distances considered in this study) the NAME plume is wider than the R91 plume. At 5 km downwind the width of the plumes are comparable, and at distances 10 km or greater downwind the R91 plume is wider than the NAME plume.

As detailed in Table 21, for a 10 degree offset in the wind direction, at distances up to and including 10 km downwind, R91-estimated time integrated activity concentrations in air are greater than respective NAME estimated values but by less than a factor of 2. At distances beyond 20 km downwind R91-estimated TIACs become progressively larger than those estimated by NAME (by up to a factor of 7 at 40 km downwind). The margin of difference observed in model estimates in the baseline model runs is greater than for a 10 degree offset in the wind direction as a result of the larger cross-wind spread of the plume in NAME (at less than 5 km downwind) which acts to increase the activity concentrations in air off axis in the y plane relative to R91 estimates or, more precisely, NAME estimated activity concentrations in air "drop off" less rapidly than R91 estimates. Conversely, the larger cross-wind spread in R91 baseline model runs at relatively large distances downwind are responsible for the divergence in model estimates of activity concentration in air for a model run assuming a 10 degree offset in wind direction (Table 21), at distances 20 km or greater downwind.

As detailed in Table 22, for a 20 degree offset in the wind direction time integrated air activity concentrations estimated by NAME are greater than those estimated by R91 at less than 5 km but converge with increasing distance downwind. The greatest disparity (a factor of 10) between estimates exists at 1 km downwind. At 10 km downwind R91 estimates of TIACs are greater than those estimated by NAME and it is envisaged that at increasing distance downwind model estimates of TIACs would diverge. Again, the reasoning for such differences is that the NAME plume is wider at relatively short distances downwind, but the R91 plume is wider at relatively large distances downwind.

The ratio of the baseline model run to a model run assuming a 10 degree offset in the wind direction increases from 1.8 at 1 km downwind to 26 at 40 km downwind for NAME model output. In comparison the ratio of the baseline model run to a model run assuming a 10 degree offset in the wind direction increases from 3.9 at 1 km downwind to 6 at 40 km downwind for R91 model output. Thus for a 10 degree error in the predicted wind direction there is smaller margin for error in the interpretation of NAME estimated TIACs at distances less than 20 km downwind and a larger margin for error in their interpretation at distances greater than 20 km downwind (relative to R91).

The ratio of the baseline model run to a model run assuming a 20 degree offset in the wind direction increases from 12 at 1 km downwind to 750 at 10 km downwind for NAME model output. In comparison, the ratio of the baseline model run to a model run assuming a 20 degree offset in the wind direction increases from 400 at 1 km downwind to 2300 at 40 km downwind for R91 model output. Thus for a 20 degree error in the predicted wind direction there is a smaller, but still very significant, margin for error in the interpretation of NAME estimated TIACs at distances less than 10 km downwind (relative to R91).

It is appreciated that large fractional differences occur in the tails of the plume and that far into the tail the differences between R91 and NAME are likely to be insignificant in absolute terms. However, within the level of uncertainty of the prediction of the direction of the wind it is relevant to this study to understand the differences between the two models and to understand the potential consequences of erroneously assuming off axis TIACs are plume centre line values.

5.8 Rainfall

5.8.1 Wet deposition

Table 23 and Table 24 show dry and wet deposition concentrations (Bq m^{-2}) as a function of distance downwind for varying precipitation rates. Input parameters were identical to those used in Section 5.1, except for changes to be consistent with a range of rainfall rates.

Table 23 NAME dry and wet deposition (Bq m^{-2}) as a function of distance downwind and precipitation

	1 km	2 km	5 km	10 km	20 km	40 km
Dry deposition	$5.2\ 10^{6}$	$2.8\ 10^{6}$	$1.3\ 10^{6}$	$7.2\ 10^{5}$	$4.0\ 10^{5}$	$2.1\ 10^{5}$
Wet deposition for precipitation of 0.5 mm hr^{-1}	$2.0\ 10^{8}$	$1.1\ 10^{8}$	$4.8\ 10^{7}$	$2.6\ 10^{7}$	$1.4\ 10^{7}$	$6.8\ 10^{6}$
Wet deposition for precipitation of 1.0 mm hr^{-1}	$3.4\ 10^{8}$	$1.8\ 10^{8}$	$8.0\ 10^{7}$	$4.3\ 10^{7}$	$2.2\ 10^{7}$	$9.9\ 10^{6}$
Wet deposition for precipitation of 2.0 mm hr^{-1}	$5.8\ 10^{8}$	$3.1\ 10^{8}$	$1.3\ 10^{8}$	$6.9\ 10^{7}$	$3.2\ 10^{7}$	$1.3\ 10^{7}$
Wet deposition for precipitation of 4.0 mm hr^{-1}	$9.9\ 10^{8}$	$5.1\ 10^{8}$	$2.1\ 10^{8}$	$1.0\ 10^{8}$	$4.3\ 10^{7}$	$1.4\ 10^{7}$
Wet deposition for precipitation of 10.0 mm hr^{-1}	$2.0\ 10^{9}$	$9.8\ 10^{8}$	$3.7\ 10^{8}$	$1.5\ 10^{8}$	$4.7\ 10^{7}$	$8.5\ 10^{6}$

Table 24 R91 ground deposition (Bq m^{-2}) as a function of distance downwind and rainfall category

	1 km	2 km	5 km	10 km	20 km	40 km
Dry deposition	$1.3\ 10^{8}$	$4.1\ 10^{7}$	$9.2\ 10^{6}$	$3.1\ 10^{6}$	$1.1\ 10^{6}$	$4.2\ 10^{5}$
Wet deposition for rainfall category LIGHT	$1.3\ 10^{9}$	$4.1\ 10^{8}$	$9.2\ 10^{7}$	$3.1\ 10^{7}$	$1.1\ 10^{7}$	$4.2\ 10^{6}$
Wet deposition for rainfall category HEAVY	$1.3\ 10^{10}$	$4.1\ 10^{9}$	$9.2\ 10^{8}$	$3.1\ 10^{8}$	$1.1\ 10^{8}$	$4.2\ 10^{7}$

It should be noted that the NAME results for wet deposition in Table 23 do not include a contribution from dry deposition (ie, they are “wet only”), whereas the R91 results for wet deposition in Table 24 do include a contribution from dry deposition (ie, they are the total ground deposition in wet conditions). However, as can be seen from Table 23 and Table 24, the values for dry deposition are sufficiently small (at most 10%) that their effects can be ignored when comparing the two sets of results.

Because of the different ways in which NAME and the method applied to R91 in this study categorise precipitation, it is not possible to make a direct comparison of the results; however, the following observations can be made. For R91 (as implemented in this study), deposition decreases with distance downwind at the same proportional rate regardless of the intensity of the rainfall (eg, (Deposition at 1 km)/(Deposition at 40 km) is the same for “HEAVY”, “LIGHT” or “NONE”). By contrast, the NAME results show a more rapid decrease with distance downwind for heavier precipitation. This is likely to be because NAME takes account of plume depletion, whereas no account was taken of this in the limited number of R91 calculations, undertaken in this study.

However, the overall rate of decrease of deposition with distance downwind is greater for the R91 results than it is for NAME; an observation which may seem counterintuitive. The reason for instinctively expecting NAME-derived deposition concentrations to decrease more rapidly than R91-derived deposition concentrations with downwind distance is due to NAME’s ability to account for plume depletion. It is evident in Section 5.8.2 that the impact of plume depletion is minimal at low rainfall rates and relatively close to the release but for high rainfall rates and downwind distances of tens of kilometres plume depletion becomes a significant factor in terms of appreciably reducing deposition downwind. Therefore, there must exist a factor more dominant in its capacity to magnify the rate of decrease of deposition with downwind distance in R91 compared with NAME.

R91-derived deposition concentrations are estimated directly from, and are therefore directly proportional to, ground level time integrated activity concentrations in air. The concentrations in air decrease at a greater rate in R91 than in NAME due to a combination of the smaller cross-wind and vertical spread of the plume in R91 at relatively small distances downwind, resulting in greater air concentrations and the larger cross-wind and vertical spread of the plume in R91 at relatively large distances downwind, resulting in more comparable air concentrations. Not only are NAME deposition concentrations not directly proportional to ground level air concentrations, but they decrease at a rate less than the decrease in NAME-estimated time integrated activity concentrations in air, which in turn decrease at a rate less than the decrease in R91-estimated time integrated activity concentrations in air.

The rate of decrease of deposition with distance downwind is likely to be greater in R91 than in NAME because the former estimates deposition concentrations on the basis of ground level time integrated activity concentrations in air, in contrast to NAME which accounts for the vertical extent of the plume in conjunction with the vertical height of the cloud and precipitation. Clearly the NAME approach is more representative of the physical processes in the atmosphere. In the near field the activity concentrations in air are relatively high but narrowly distributed in the vertical such that any precipitation has only a limited opportunity to washout the radioactivity. Further downwind the radioactivity is more widely dispersed in the vertical and is therefore at lower activity concentrations, but there is more of an opportunity for precipitation to washout the radioactivity. As the plume disperses downwind, the decrease in the activity concentration in air is still the dominant factor in determining the pattern of deposition, but the greater washout (and potentially rainout) efficiency results in a degree of counterbalancing of deposition concentrations, acting to reduce the concentration gradient with distance in NAME. No account is made in R91 of the increasing washout efficiency of precipitation with increasing distance downwind (ie, as the plume becomes more widely spread in the vertical).

Precipitation of 10 mm hr^{-1} was considered to be a suitable upper bound for the NAME runs because it is representative of very heavy but potentially persistent rainfall over periods of tens of minutes and possibly (in extreme circumstances) up to an hour or so in the UK. The degree of wet deposition associated with a precipitation rate of 10 mm hr^{-1} in NAME is significantly lower than for an R91 model run assuming “heavy” rainfall (even when accounting for the relative difference in the time integrated activity concentrations in air, Table 9). This is likely to be a feature of the specific approach implemented in R91 in this study, rather than of R91 *per se*. Specifically, these results suggest that the R91 approach is conservative in its estimation of the effects of heavy rainfall on deposition, ie, estimates of deposition concentrations in heavy rain are significantly greater than would typically be expected under such conditions.

The Met Office (Met Office, 2010) website defines “slight” rainfall as 0.5 to 1 mm hr^{-1} and “moderate” rainfall as 1 to 4 mm hr^{-1} (with the next category above 4 mm hr^{-1} being “heavy”). It is reasonable to interpret this to mean that “light” rainfall is approximately

1 mm hr^{-1}. The ratio of R91 estimates of ground deposition in LIGHT rainfall to NAME estimates of wet deposition in precipitation of 1.0 mm hr^{-1} is 3.8 at 1 km downwind, decreasing steadily to 0.4 at 40 km downwind. Hence, for “light” rainfall and short distances downwind, R91 (as implemented in this study) predicts greater deposition than NAME, whereas for “light” rainfall and large distances downwind, NAME predicts greater deposition than R91.

5.8.2 Plume depletion

R91, as applied in this study, does not include plume depletion. The NAME baseline model run assumes no deposition and therefore no plume depletion, thus enabling a fairer comparison with R91. This section investigates how NAME model estimates of time integrated air activity concentration are likely to vary when accounting for plume depletion. The number of particles used in NAME to describe the atmospheric dispersion of the plume was reduced for model runs investigating plume depletion (from 1 million to 10,000) to reduce model run time. This increased the influence of statistical noise on model output. For this reason, the estimated time integrated air activity concentrations in dry conditions (Table 25) do not exactly match those derived in the baseline model run (Table 9). Also, no time integrated air activity concentrations are estimated at 40 km downwind (Table 25).

Plume depletion starts to become significant (where “significant” implies a difference of a factor of two or more in plume centre line TIACs) only at distances of 10 km or more downwind for rainfall rates of 10 mm hr^{-1} and at distances of 20 km or more downwind for rainfall rates of 4 mm hr^{-1}. At 20 km downwind, assuming a rainfall rate of 10 mm hr^{-1}, plume depletion results in a factor of 4 reduction in time integrated air activity concentrations. A precipitation rate of 10 mm hr^{-1} is representative of very heavy but potentially persistent rainfall over periods of tens of minutes and possibly (in extreme circumstances) up to an hour or so. A downpour is described as greater than 16 mm hr^{-1} (Met Office, 2010) and is likely to be a very localised event lasting of the order of minutes only.

Table 25 NAME ground level time integrated activity concentrations in air (Bq s m^{-3}) as a function of distance downwind and precipitation

	1 km	2 km	5 km	10 km	20 km
TIAC for dry conditions	$4.6\ 10^{10}$	$1.4\ 10^{10}$	$4.2\ 10^{9}$	$1.8\ 10^{9}$	$1.8\ 10^{9}$
TIAC for precipitation of 0.5 mm hr^{-1}	$4.5\ 10^{10}$	$1.4\ 10^{10}$	$4.1\ 10^{9}$	$1.7\ 10^{9}$	$1.6\ 10^{9}$
TIAC for precipitation of 1.0 mm hr^{-1}	$4.5\ 10^{10}$	$1.4\ 10^{10}$	$4.0\ 10^{9}$	$1.6\ 10^{9}$	$1.4\ 10^{9}$
TIAC for precipitation of 2.0 mm hr^{-1}	$4.5\ 10^{10}$	$1.4\ 10^{10}$	$3.8\ 10^{9}$	$1.5\ 10^{9}$	$1.2\ 10^{9}$
TIAC for precipitation of 4.0 mm hr^{-1}	$4.4\ 10^{10}$	$1.3\ 10^{10}$	$3.5\ 10^{9}$	$1.3\ 10^{9}$	$8.9\ 10^{8}$
TIAC for precipitation of 10.0 mm hr^{-1}	$4.2\ 10^{10}$	$1.2\ 10^{10}$	$2.9\ 10^{9}$	$8.8\ 10^{8}$	$4.2\ 10^{8}$

To give an illustration of the variation of plume depletion with precipitation, Table 26 details the ratio of time integrated activity concentration in air accounting for varying rates of precipitation to the time integrated activity concentration in air under dry conditions at 20 km downwind.

Table 26 Ratio of ground level time integrated activity concentrations in air as a function of precipitation at 20 km downwind

	0.0 mm hr^{-1}	0.5 mm hr^{-1}	1.0 mm hr^{-1}	2.0 mm hr^{-1}	4.0 mm hr^{-1}	10.0 mm hr^{-1}
(TIAC including precipitation) / (TIAC assuming zero precipitation)	1.0	0.87	0.79	0.67	0.49	0.24

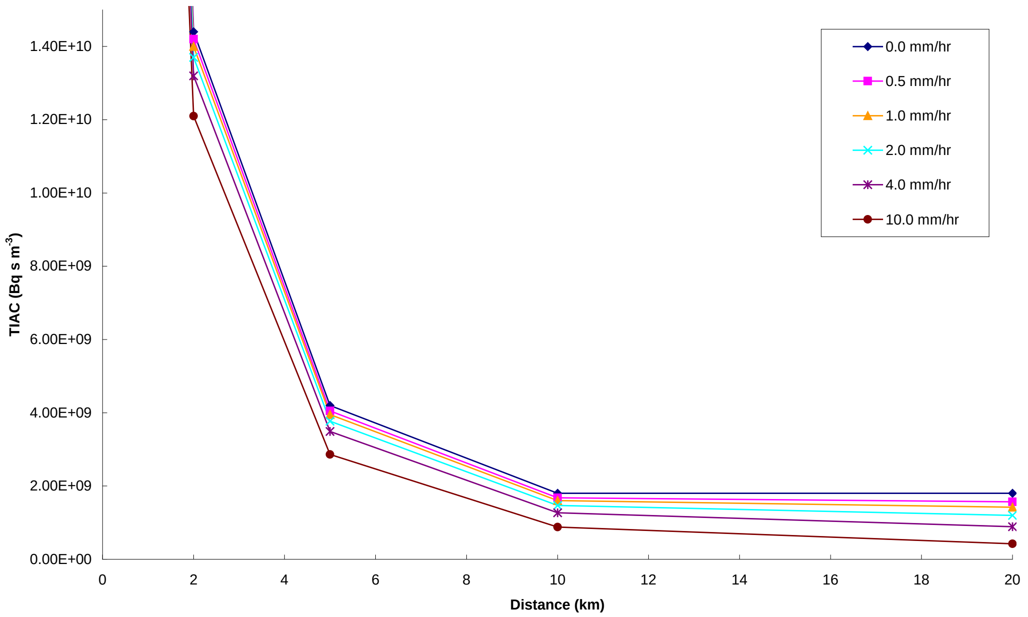

Figure 20 Ground level time integrated activity concentrations in air (Bq s m^{-3}) as a function of distance downwind and precipitation rate

It is evident from Figure 20 that the rate of decrease of time integrated activity concentration in air at a given distance downwind varies smoothly with rate of precipitation, with no obvious "threshold" rate at which plume depletion increases suddenly.

5.9 Combination of amendments to the baseline model run

Clarke (1979) states that dispersion calculations may be best represented by wind speeds at the height of the plume centre line, or the mean wind speed through the depth of the plume, but suggests that use of a single wind speed at a height of 10 m above the ground is often appropriate. This is on the basis that in the recommended Gaussian model the denominator of the equation used to estimate activity concentration in air contains the product of u and σ_y and whilst u increases with increasing height, σ_y decreases with increasing height. This section investigates the difference in R91 and NAME output for a range of atmospheric conditions and release heights and assesses the potential improvement (or otherwise) in the R91 output as a result of considering a more representative wind speed, for example at the height of the Gaussian plume centre line (ie, the release height for a non-buoyant release) or at the height of the mean wind speed through the depth of the plume (see Section 4.3 for details of the different methods assumed in R91 and NAME for modelling wind speed). Note that in all cases where R91 assumes a wind speed at an alternate height to 10 m, the meander term of the cross-wind spread of the plume is modified to reflect this.

5.9.1 Unstable conditions combined with a range of release heights

Table 27 and Table 28 apply to Pasquill stability category A conditions which assume a typical boundary layer depth of 1300 m, and a wind speed of 1 m s^{-1} at 10 m above ground level. The default NAME and R91 model output detailed in Table 27 assume a release height of 10 m and in Table 28 assume a release height of 200 m. The height of the assumed wind speed in R91 may be modified either by considering the mean wind speed through the depth of the plume or a single wind speed at the height of the plume centre line. For both release heights and all distances downwind shown in Table 27 and Table 28, these modifications result in an improved agreement between the R91 and NAME estimated activity concentrations in air. It is recognised that this approach will overemphasise the effect at all distances downwind, more significantly at larger distances; however, the approach is still indicative of the likely effect (see Section 4.3 for details). For a release at 10 m above ground level, modifying the height of the assumed wind speed to the height of the mean wind speed through the depth of the plume in R91 reduces the difference between R91 and NAME estimated time integrated activity concentrations in air from a factor of 30, 6.9 and 2.6 to a factor of 10, 2.6 and 1.2 at 1, 5 and 40 km downwind, respectively. Similarly, for a release at 200 m above ground level, modifying the height of the assumed wind speed in R91 reduces the difference between R91 and NAME estimated time integrated activity concentrations in air from a factor of 15, 6.5 and 2.8 to a factor of 5.4, 2.8 and 1.2 at 1, 5 and 40 km downwind, respectively. For a 200 m release height, the differences between R91 and NAME estimates are the same irrespective of whether the R91 model is amended to consider a single wind speed at the height of the plume centre line or the mean wind speed through the depth of the plume. It is perhaps intuitive that the wind speed at a few 100 m would be more representative than that at 10 m for a release at a height of 200 m, but less so for a release height of 10 m. For a release height of 10 m in unstable conditions, released material soon spreads through the vertical extent of the boundary layer. The vertical domain is bounded by the ground and therefore a low level release predominantly spreads upwards. In unstable atmospheric conditions, as considered here, there exists a large degree of mixing and therefore very quickly the plume will spread over a large vertical extent of the boundary layer, to heights much greater than 10 m. Under such circumstances a large percentage of the plume will travel downwind at heights significantly greater than 10 m, thus justifying the application of a modified wind speed representative of a much greater height than the 10 m release height assumed.

Contrary to Clarke (1979), it is evident in Table 27 and Table 28 that for estimates of activity concentration in air in unstable conditions, increases in u with increasing height are not counterbalanced by decreases in σ_y with increasing height and in fact any increase in u dominates, resulting in an overall decrease in activity concentrations in air.

Table 27 Ground level time integrated activity concentrations in air (Bq s m^{-3}) as a function of distance downwind; for a large boundary layer depth, release height 10 m and Pasquill stability category A

	1 km	5 km	40 km
NAME model run	$2.3\ 10^{9}$	$5.4\ 10^{8}$	$1.4\ 10^{8}$
R91 model run	$6.9\ 10^{10}$	$3.7\ 10^{9}$	$3.6\ 10^{8}$
R91 model run, amended for single wind speed at the height of the mean wind speed through the depth of the plume	$2.3\ 10^{10}$	$1.4\ 10^{9}$	$1.2\ 10^{8}$

Table 28 Ground level time integrated activity concentrations in air (Bq s m^{-3}) as a function of distance downwind; for a large boundary layer depth, release height 200 m and Pasquill stability category A

	1 km	5 km	40 km
NAME model run	$2.4\ 10^{9}$	$5.4\ 10^{8}$	$1.3\ 10^{8}$
R91 model run	$3.5\ 10^{10}$	$3.5\ 10^{9}$	$3.6\ 10^{8}$
R91 model run, amended for single wind speed at height of the plume centre line	$1.3\ 10^{10}$	$1.6\ 10^{9}$	$1.6\ 10^{8}$
R91 model run, amended for single wind speed at the height of the mean wind speed through the depth of the plume	$1.3\ 10^{10}$	$1.5\ 10^{9}$	$1.5\ 10^{8}$

The difference in time integrated activity concentrations in air between NAME and R91 for a release 10 m above ground level (Table 27) is greater than for a release at 200 m above ground level (Table 28), which may at first appear to be counterintuitive. However, as explained in Section 5.2, it is likely that R91 typically estimates the spread of the plume to be less than reality, therefore estimates of time integrated activity concentrations in air are a factor of 30 greater than those estimated by NAME at 1 km downwind for a release 10 m above ground level. A similar under-prediction of plume spread is likely in R91 for a release at 200 m above ground level but as a result, a release at height is likely to take longer to reach the ground in R91, and more to the point, impinge on the ground further downwind, thus reducing the magnitude of the difference in time integrated activity concentrations in air between approaches (to a factor of 15).

5.9.2 Stable conditions combined with a range of release heights

Table 29 and Table 30 apply to Pasquill stability category G conditions which assume a typical boundary layer depth of 100 m (and a wind speed of 1 m s^{-1} at 10 m above ground level). The default NAME and R91 model output detailed in Table 29 assume a release height of 10 m and in Table 30 assume a release height of 90 m.

For a release height of 10 m above ground level and for all distances downwind, considered in this study, modifying the height of the assumed wind speed in R91 by considering the mean wind speed through the depth of the plume results in an improved agreement between R91 and NAME estimated activity concentrations in air. It is recognised that this approach will overemphasise the effect at all distances downwind, more significantly at larger distances; however, the approach is still indicative of the likely effect (see Section 4.3 for details). An explanation for the improved agreement between R91 and NAME estimated activity concentrations in air can be found in Section 5.9.1. Consideration of a single wind speed at the height of the plume centre line gives analogous results and therefore has been omitted in this study for brevity.

For a release height 90 m above ground level the margin of difference in time integrated activity concentrations in air estimated by NAME and R91 is very large at 5 km and even greater at 1 km downwind. In the near field, estimates of time integrated activity concentrations in air using R91 are significantly smaller than those estimated in NAME because the release is mixed down to the ground much less rapidly in R91. However, at 40 km downwind estimates of time integrated activity concentration in air using R91 are greater than those estimated in NAME because the main body of the plume modelled by R91 has reached the ground and there is less horizontal spread of the plume assumed by R91.

Amending the default R91 model run to account for the mean wind speed through the depth of the plume acts to reduce estimated time integrated activity concentrations in air at all distances downwind (considered in this study). This is because the affect of increasing the wind speed outweighs the converse affect of decreasing the standard deviation of the cross-wind profile of the plume, ie, the denominator of the R91 Gaussian plume model equation is larger for the R91 amended model run.

Amending the default R91 model run to account for the mean wind speed through the depth of the plume improves the agreement between R91 and NAME model output at 40 km but exacerbates the difference at 1 and 5 km downwind, however in all cases the impact is marginal and insignificant. It is likely that modifying the assumed height of the wind speed to a value more representative of the height of the mean wind speed through the depth of the plume would improve estimates of time integrated activity concentration in air using R91; however, evidence of this is obscured by a much more dominant effect resulting from a difference between approaches in the description of the vertical spread of the plume with height in very stable conditions, especially at relatively short distances from a release.

Table 29 Ground level time integrated activity concentrations in air (Bq s m^{-3}) as a function of distance downwind; for a small boundary layer depth (100 m), release height 10 m and Pasquill stability category G

	1 km	5 km	40 km
NAME model run	$1.6\ 10^{11}$	$1.7\ 10^{10}$	$1.2\ 10^{9}$
R91 model run	$1.0\ 10^{12}$	$1.5\ 10^{11}$	$8.3\ 10^{9}$
R91 model run, amended for single wind speed at the height of the mean wind speed through the depth of the plume	$7.6\ 10^{11}$	$1.1\ 10^{11}$	$5.0\ 10^{9}$

Table 30 Ground level time integrated activity concentrations in air (Bq s m^{-3}) as a function of distance downwind; for a small boundary layer depth (100 m), release height 90 m and Pasquill stability category G

	1 km	5 km	40 km
NAME model run	$6.1\ 10^{8}$	$4.8\ 10^{9}$	$9.6\ 10^{8}$
R91 model run	$2.9\ 10^{-17}$	$2.0\ 10^{7}$	$3.3\ 10^{9}$
R91 model run, amended for single wind speed at the height of the mean wind speed through the depth of the plume	$1.8\ 10^{-17}$	$1.3\ 10^{7}$	$2.4\ 10^{9}$

Note that under very stable atmospheric conditions, time integrated activity concentrations in air estimated by R91 can vary significantly as a result of moderate changes in release height. For example assuming a 70 m release height in R91 implies time integrated activity concentrations in air of $3.2\ 10^{-5}$, $8.9\ 10^{8}$ and $4.1\ 10^{9}$ Bq s m^{-3} estimated at 1, 5 and 40 km downwind, respectively. Therefore under very stable atmospheric conditions it is important that the model release height assumed is an accurate reflection of the true state of the release.

6 MODIFICATIONS TO THE NAME BASELINE MODEL RUN AND THEIR IMPLICATIONS

The purpose of this study was to analyse the differences between R91 and NAME in the context of emergency assessment scenarios. To perform such an intercomparison objectively all user defined variables were set such that an evaluation of the two models would compare like with like. Furthermore, all scenarios were defined to suit the application of both models, notably flat terrain and steady state meteorological conditions. As a result the form of the NAME model run was simplistic, and functionality with the potential to enhance the ability to model dispersion was left redundant. If NAME were to be used to perform an emergency assessment it is likely that it would not be applied in the same fashion as in this study (see Sections 3-5). This section considers the functionality in NAME not considered in this study but which could be an asset if running NAME in an emergency response capacity.

NAME has the capability to consider multiple releases and variable release rates in contrast to HPA's application of R91 which can only consider a single release at a constant release rate. In principle R91 could consider multiple releases by adding together the individual contributions.

NAME applies random walk formulae to determine the turbulent velocity components in both the horizontal and the vertical. NAME considers two schemes, of varying complexity and computational expense, in the estimation of near-source diffusion. The baseline model run assumed the simplified scheme as a result of its suitability for comparison with R91. The "near source scheme" is more advanced in its capabilities to model dispersion but is also more computationally expensive. Setting the "Velocity Memory Time" and "Inhomogeneous Time" to non-zero positive values initiates the use of the near source scheme in the first few minutes after the material is released, which then reverts to the (computationally) cheap scheme at greater travel times from the source. The near source scheme applies the full random walk specification for appropriate values of the (inhomogeneous) profiles of the horizontal and vertical turbulent velocity variances, and the horizontal and vertical Lagrangian timescales, which are determined from empirical fits to observational data, combined with information available from the Unified Model, including the friction velocity, boundary layer depth, convective velocity and surface heat flux. The random walk formulae for turbulent velocity components is applied for the near source scheme, including a term representing memory of previous motion and a term representing a new random perturbation. The near source scheme can be particularly useful when modelling more complex dispersion processes near to the source of the release, such as plume rise. The cheap scheme for determining turbulent velocity components in the vertical (applied in this study) assumes a simple constant diffusion coefficient scheme which is somewhat limited in its ability to replicate the turbulent behaviour as modelled by the more complex near source scheme; consequently there exists the potential for differences in endpoints as a result of the modelling approach assumed. In NAME setting the “Skew Time” to a non-zero positive value is likely to further improve the turbulence profile but only in convective, unstable conditions. In this instance the velocity standard deviations and time scales are the same as the inhomogeneous profiles, but in addition a non-zero third order moment of vertical velocity is assumed.

NAME can account for the temporal and spatial variability observed in the meteorology which describes the atmosphere. Thus for single site data NAME accounts for temporally varying meteorological data and can also consider temporally and spatially varying gridded meteorological data from Numerical Weather Prediction (NWP) models. In contrast R91 assumes single-site steady-state meteorological conditions with no time or space variation. This implies many potential differences between NAME and R91 model estimates. R91 as applied by HPA assumes a single wind direction and no variability in direction as a result of the meteorological data provided (R91 does account for variability in wind direction as a result of meander and turbulence however); therefore typically NAME plumes will tend to be wider, especially for a release lasting a number of hours. Also R91 assumes that if it is raining, the entire plume is affected at the same rainfall rate and therefore the activity concentrations deposited will be uniformly distributed; however, NAME deposition is likely to demonstrate a more realistic distribution including concentration spikes and hotspots. Fine-scale detail may not be reliable due to issues of predictability at the grid scale of NWP models; however, radar rainfall estimates are likely to be more reliable.

NAME models explicitly the temporal evolution of a plume and accounts for the time taken for the plume to reach each grid point. In contrast R91, as detailed in the NRPB-R91 report (Clarke, 1979) and applied in this study, assumes instantaneous travel of the plume and therefore calculates the total eventual time integrated air concentration at each point in space. Because of such differences in modelling, the NAME results show a source to receptor distance dependence that means that receptors at different distances reach steady-state activity concentrations in air at different times. R91, as detailed in the NRPB-R91 report (Clarke, 1979) and implemented in this study, also does not consider radioactive decay during plume travel, in contrast to NAME.

NAME can account for a variety of particle sizes (and particle densities) and as a result can account for gravitational settling. R91 was developed specifically for gases but the method applied is applicable to small particles, most notably particles 1 micron or less in size. In general R91 should not be used to model particles larger than 10 microns in size and does not account for gravitational settling.

NAME can model atmospheric dispersion in complex terrain by coupling with the LINCOM model (Astrup, 1996). NAME can consider a range of roughness lengths to describe different land use and separate roughness lengths can be considered for the release site and meteorological site. In contrast the method applied in R91 within this study (and in HPA's application of R91 for emergency assessments) is limited to the consideration of a single roughness length of 0.3 m, representative of a rural area and agricultural land use.

7 CONCLUSIONS

This report compares the predictions of the R91 model as applied by HPA for emergency response assessments with those of NAME. Model comparisons between R91 and NAME are centred upon the analysis of model output generated from a single baseline run, representing a short duration release. There is a disparity (of up to a factor of approximately 3) between those plume centre line time integrated activity concentrations in air (TIACs) derived using NAME and those derived using R91, most notably in the near-field. In the range 1 to 40 km downwind the maximum TIAC estimated by R91 is greater than that estimated by NAME. The cross-wind spread of the plume, vertical spread of the plume and wind-driven advection of the plume were identified as potential sources of the observed differences between R91 and NAME model output. Analysis of the contribution from these three parameters indicated that they are all partially responsible for the differences and cumulatively explain the majority, if not all, of the differences in the observed model output.

It is apparent that the scientific principles behind the modelling in NAME and more specifically behind the modelling of the cross-wind spread of the plume, the vertical spread of the plume and the advection of a plume downwind are more representative and robust than those in R91. However, model validation is not readily available in all cases to substantiate this.

The quantitative assessment of differences in output from the NAME and R91 baseline model run is used as part of a qualitative assessment of observed differences in model output across a range of scenarios. The key observations are highlighted below.

a) There are significantly larger differences in TIACs derived by NAME and R91 for Pasquill stability category A and G conditions than for the baseline Pasquill stability category D model run.

b) There are much larger differences in TIACs at 1 km downwind derived by NAME and R91 for large release heights (80 and 200 m) than for the baseline 10 m release height model run.

c) There are large differences in TIACs derived by NAME and R91 for low wind speeds (0.1, 0.5, 0.8 and 1.0 m s^{-1}) in stable and unstable conditions compared to the baseline model run assumption of a 5 m s^{-1} wind speed in neutral stability conditions.

d) Differences in TIACs derived by NAME and R91 for high wind speeds (10 and 15 m s^{-1}) are comparable to those observed for the baseline model run assumption of a 5 m s^{-1} wind speed.

e) Differences in TIACs derived by NAME and R91 for variable release durations (4, 8 and 12 hours) are comparable to those observed for the baseline model run assumption of a 1-hour release. TIACs estimated by R91 decrease with increasing release duration. In contrast TIACs estimated by NAME are not a function of release duration (at least for those durations considered here).

f) Differences in TIACs derived by NAME and R91 for a 10 degree offset in the wind direction are comparable to those observed for the baseline model run. However, for a 20 degree offset in the wind direction there exist large differences in TIACs derived by NAME and R91 compared to the baseline model run.

g) It was not possible to make a direct comparison between wet deposition concentrations derived by NAME and R91, because of the latter's qualitative description of rainfall intensity; however, R91 is clearly conservative in its assumptions, primarily in its application of deposition velocities and washout; for example estimates of deposition concentrations in heavy rain are significantly greater than would typically be expected under such conditions.

h) The impact of plume depletion on TIACs estimated by NAME during light rain (1 mm hr^{-1}) was not significant for any distance downwind considered in this study. Plume depletion starts to become significant in heavy rain (10 mm hr^{-1}) at distances of 10 km or greater downwind.

Future work could assess the reasons for the differences observed between R91 and NAME in the additional runs performed here, primarily by focusing on the contributions from the cross-wind spread of the plume, vertical spread of the plume and wind-driven advection, as performed for the baseline model run in this study.

8 REFERENCES

Astrup P (1996). LINCOM user guide for version L1. Risø National Laboratory, DK-4000, Roskilde, Denmark, RODOS(WG2)-TN(96) 07:17.

Atmospheric Dispersion Modelling Liaison Committee (ADMLC) (1997). Annual Report 1995/1996. Chilton NRPB-R292.

Atmospheric Dispersion Modelling Liaison Committee (ADMLC) (1999). Annual Report 1996/1997. Chilton, NRPB-R302.

Barad ML (1958). Project Prairie Grass, a field program in diffusion. Geophys Res Pap, 59. Air Force Cambridge Centre.

Bowne NE and Londergan RJ (1983). Overview, results and conclusions for the EPRI plume model validation and development project: plains site. EPRI report EA-3074.

Carruthers DJ, Edmunds HA, Bennett M, Woods PT, Milton MJT, Robinson R, Underwood BY and Franklin CJ (1996). Validation of the UK-ADMS Dispersion Model and Assessment of its Performance relative to R91 and ISC using Archived LIDAR Data. DoE/HMIP Report No DoE/HMIP/RR/95/022.

Clarke RH (1979). The first report of a Working Group on Atmospheric Dispersion: a model for short and medium range dispersion of radionuclides released to the atmosphere. Chilton, NRPB-R91.

CERC (2010). Boundary layer structure specification. P09/01V/10.

Crawford TV (1978). Atmospheric Transport of Radionuclides, IN Proceedings of a Workshop on the Evaluation of Models Used for the Environmental Assessment of Radionuclide Releases, pp 5-32. FO Hoffman, DL Shaeffer, CW Miller and CT Garten Jr (Eds). DOE Report CONF-770901, NTIS.

Davies BM and Thomson DJ (1999). Comparison of some parameterizations of wind direction variability with observations. Atmospheric Environ, 33 (29), 4909-4917.

Gifford FA (1968). Diffusion in the lower layers of the atmosphere. IN Meteorology and Atomic Energy (D Slade, Ed). US Atomic Energy Commission, TID-24190, p65.

Hanna SR, Briggs GA, Deardorff J, Egan BA, Gifford Jr FA and Pasquill F (1977). AMS Workshop on Stability Classification Schemes and Sigma Curves – Summary of Recommendations. Bull Am Meteorol Soc, 58 (12), 1305-1309.

Jones A, Thomson D, Hort M and Devenish B (2007). The UK Met Office's next generation atmospheric dispersion model NAME III. Air Pollution Modelling and its Application XVII. Eds: C Borrego and A-L Norman. Berlin: Springer.

Jones JA (1981). The second report of a Working Group on Atmospheric Dispersion: a procedure to include deposition in the model for short and medium range atmospheric dispersion of radionuclides. Chilton, NRPB-R122.

Jones JA (1983). The fifth report of a Working Group on Atmospheric Dispersion: models to allow for the effects of coastal sites, plume rise and buildings on dispersion of radionuclides and guidance on the value of deposition velocity and washout coefficients. Chilton, NRPB-R157.

Jones JA, Mayall A, Cooper PJ and Davies T (1995). Comparison of the ADMS and R91 atmospheric dispersion models. Chilton, NRPB-M572.

Kretzschmar JG, Mertens I, De Baere G and Vandervee J ((1983). Influence of the turbulence typing scheme upon the cumulative frequency distributions of the calculated relative concentrations for different averaging times. European Commission, Brussels, EUR-8478.

Kretzschmar JG, Mertens I and Vanderborght B (1984). Sensitivity, applicability and validation of bi-gaussian off- and on-line models for the evaluation of the consequences of accidental releases in nuclear facilities. European Commission, Brussels, EUR-9385.

Lowles I (2002). Model comparison and uncertainty. AQMAU Model uncertainty workshop.

Maryon RH (1998). Determining cross-wind variance for low-frequency wind meander. Atmospheric Environ, 32 (2), 115-121.

Maryon RH, Ryall DB and Malcolm AL (1999). The NAME 4 Dispersion Model: Science Documentation. Met O (PMSR) Turbulence and Diffusion Note No 262.

Met Office (2010). http://www.metoffice.gov.uk/weather/uk/guide/key.html#radar

Miller CW and Hively LM (1987). A review of validation studies for the Gaussian Plume Atmospheric Dispersion Model. Nucl Safety, 28 (4).

Moore DJ (1976). Calculation of ground level concentration for different sampling periods and source locations. IN Atmospheric Pollution. Amsterdam, Elsevier, p 5160.

Panofsky HA and Dutton A (1984). Atmospheric Turbulence. Wiley.

Pasquill F (1974). Atmospheric Diffusion. 2nd Ed. John Wiley and Sons, New York.

Pasquill F and Smith FB (1983). Atmospheric Diffusion, study of the dispersion of windborne material from industrial and other sources, 3rd Ed. John Wiley & Sons Ltd, New York.

Ryall DB and Maryon RH (1998). Validation of the UK Met Offices NAME model against the ETEX dataset. Atmospheric Environ, 32 (24), 4265-4276.

Smith FB (1973). A scheme for estimating the vertical dispersion of a plume from a source near ground level. IN Proc. 3rd Meeting of an Expert Panel on Air Pollution Modelling. Paris, October, 1972. Brussels, NATO-CCMS Report 14.

Thomson DJ and Jones AR (2011). A new puff modelling technique for short range dispersion applications. Int J Environment and Pollution, Vol (TBC).

Thomson DJ and Manning AJ (2001). Along wind dispersion in light wind conditions. Boundary-Layer Meteorology, 98, 341–358.

Van Ulden AP and Holtslag AAM (1985). Estimation of atmospheric boundary layer parameters for diffusion applications. J Clim Appl Met, 24, 1194-1207.

Vogt K (1977). Empirical investigations of the diffusion of waste air plumes in the atmosphere. Nucl Tech, 34.

Weber AH (1976). Atmospheric Dispersion Parameters in Gaussian Plume Modelling: Part I. Review of Current Systems and Possible Future Developments, EPA Report EPA-600/4-76-030a, Environmental Protection Agency, NTIS.

Webster HN and Thomson DJ (2005). Parameterising low-frequency meander in atmospheric dispersion models. Proceedings of the 10th International Conference on Harmonisation within Atmospheric Dispersion Modelling for Regulatory Purposes, eds. AN Skouloudis, P Kassomenos and J Bartzis, 594-598.

APPENDIX A

Glossary

A1 ACRONYMS AND TERMS

A1.1 ACRONYMS

ADMS	Atmospheric Dispersion Modelling System
AMAD	Activity median aerodynamic diameter
CERC	Cambridge Environmental Research Consultants
HPA	Health Protection Agency
LIDAR	Light detection and ranging
NAME	Numerical atmospheric-dispersion modelling environment
NRPB	National Radiological Protection Board
NWP	Numerical weather prediction
PCL	Plume centre line
R91	Gaussian plume model as detailed in Clarke (1979)
TIAC	Time integrated activity concentration in air

A1.2 Scientific Terminology

A	Depth of mixing layer (m)
C(x, y, z)	Time integrated air concentration (Bq s m^{-3})
F(h, z A)	A term for the vertical distribution of activity in a Gaussian plume
h	Effective release height (m)
k	Von Karman's constant
L_{MO}	Monin-Obukhov length (m)
Q	Total activity released (Bq)
T	Release duration (h)
u	Wind speed (m s^{-1})
u_{10}	Wind speed at a height of 10 m (m s^{-1})
u_*	Friction velocity (m s^{-1})
x	Rectilinear co-ordinates along the mean wind direction (m)
y	Rectilinear co-ordinates horizontally at right angles to the mean wind direction (m)
z	Rectilinear co-ordinates vertically (m)
z_o	Ground roughness length (m)
μ	'Mean value'
σ_y	Standard deviation of the cross-wind Gaussian plume profile (m)
σ_{yt}	Standard deviation of the cross-wind Gaussian plume profile due to turbulent diffusion (m)
σ_{yw}	Standard deviation of the cross-wind Gaussian plume profile due to fluctuations in wind direction (m)
σ_z	Standard deviation of the vertical Gaussian plume profile (m)
$\sigma_{z,reflected}$	Standard deviation of the reflected vertical Gaussian plume profile (m)
$\sigma_{z,unreflected}$	Standard deviation of the unreflected vertical Gaussian plume profile (m)

APPENDIX B

Outline of the R91 Gaussian plume model approach implemented in HPA's emergency response tool

The implementation of R91 in this study assumes the R91 Gaussian plume model equation (equation B1) with the inclusion of virtual sources (equation B2) characterising the impact of the ground and atmospheric boundary layer top on activity concentrations in air (Clarke, 1979).

The time integrated activity concentration in air on the plume centre line at ground level is:

$$C(x,y,z) = Q\frac{1}{2\pi\sigma_y\sigma_z u_{10}} e^{\left(\frac{-y^2}{2\sigma_y^2}\right)} F(h,z,A) \qquad \text{B1}$$

where

$$F(h,z,A) = e^{\left(\frac{-(z-h)^2}{2\sigma_z^2}\right)} + e^{\left(\frac{-(z+h)^2}{2\sigma_z^2}\right)} + e^{\left(\frac{-(2A+z+h)^2}{2\sigma_z^2}\right)} + e^{\left(\frac{-(2A+z-h)^2}{2\sigma_z^2}\right)} + e^{\left(\frac{-(2A-z+h)^2}{2\sigma_z^2}\right)} + e^{\left(\frac{-(2A-z-h)^2}{2\sigma_z^2}\right)}$$

B2

where

C (x, y, z) is the time integrated activity concentration in air (Bq s m^{-3}) over the release period at downwind distance x (m), cross-wind distance y (m) and vertical distance z (m)

Q is the total amount of activity released (Bq)

σ_y and σ_z are the standard deviations of the horizontal and vertical plume at distance x (m)

u_{10} is the windspeed at a height of 10 m (m s^{-1})

h is the release height (m)

A is the depth of the boundary layer (m).

When material is discharged from an elevated source the plume will spread vertically until the lower part reaches the ground and the upper part reaches the boundary layer top. There is then a restriction on the downward and upward diffusion, respectively. The actual vertical distribution of activity is well represented by assuming that the plume is reflected off the ground and boundary layer top back into the boundary layer. This is accounted for by the term, F(h, z, A). In this study this term accounts for five reflections, three off the ground and two off the top of the boundary layer. For the dispersion scenarios and model output considered in this study five reflection terms provide sufficient modelling accuracy.

The equation for σ_y is:

$$\sigma_y^2 = \sigma_{yt}^2 + \sigma_{yw}^2 \qquad \text{B3}$$

where

σ_{yt} is the component of σ_y due to turbulent diffusion (m)

σ_{yw} is the component of σ_y due to fluctuations in the wind direction (m).

The σ_{yw} term is approximated by:

$$\sigma_{yw} = 0.065x\sqrt{\left(\frac{7T}{u}\right)} \qquad \text{B4}$$

where

T is the release duration (hours).

No formulae are used to describe σ_{yt} and σ_z in R91 as applied in this study. Both parameters are derived purely on the basis of empirical data from Gifford (1968) and Smith (1973) respectively.

References

Clarke RH (1979). The first report of a Working Group on Atmospheric Dispersion: a model for short and medium range dispersion of radionuclides released to the atmosphere. Chilton, NRPB-R91.

Gifford FA (1968). Diffusion in the lower layers of the atmosphere. IN Meteorology and Atomic Energy (D Slade, Ed). US Atomic Energy Commission, TID-24190, p 65.

Smith FB (1973). A scheme for estimating the vertical dispersion of a plume from a source near ground level. IN Proc. 3rd Meeting of an Expert Panel on Air Pollution Modelling. Paris, October, 1972. Brussels, NATO-CCMS Report 14.

APPENDIX C

Estimating the cross-wind and vertical standard deviations of the plume using NAME model output

C1 ESTIMATING THE CROSS-WIND STANDARD DEVIATION OF THE PLUME USING NAME MODEL OUTPUT

Cross-wind profiles of TIACs were estimated using NAME at 1, 2, 5, 10, 20 and 40 km downwind, from which estimates of σ_y were generated for comparison with R91 derived values of the standard deviation of the cross-wind Gaussian plume profile.

The distribution in the TIACs is a full Gaussian curve in the cross-wind direction for R91 (equation C1a and C1b). For details of the terminology in the equations highlighted below refer to Appendix A, Table 1.2. The concentration of this curve is:

$$C(y) = e^{\left(\frac{-y^2}{2\sigma_y^2}\right)} \qquad \text{C1a}$$

The normalised concentration of this curve is:

$$C(y) = \frac{1}{\sqrt{2\pi}\sigma_y} e^{\left(\frac{-y^2}{2\sigma_y^2}\right)} \qquad \text{C1b}$$

The standard deviation of the cross-wind Gaussian plume profile is:

$$\sigma_y^2 = \frac{\int (y - \bar{y})^2 C(y) dy}{\int C(y) dy} \qquad \text{C2}$$

The mean value of the cross wind (y) co-ordinate for the data points considered:

$$\bar{y} = \frac{\int yC(y)dy}{\int C(y)dy} \qquad \text{C3}$$

Equations C2 and C3 were used to estimate the cross-wind profiles of time integrated activity concentration in air from NAME model output for comparison with the equivalent values assumed in R91.

C2 ESTIMATING THE VERTICAL STANDARD DEVIATION OF THE PLUME USING NAME MODEL OUTPUT

Calculating σ_z is a little more complex because of the presence of the ground (and the boundary layer). In R91 the vertical standard deviation of the plume is assumed to be Gaussian or normally distributed and this would be the case if there were no reflections off the ground (and the boundary layer top). However as a release disperses downwind it will interact with the ground and R91 assumes it is reflected back into the atmosphere. This reflection distorts the classic Gaussian distribution profile. R91 does not account for this by altering the value of σ_z but instead considers additional exponential terms (which are a function of height above the ground, z, effective release height, h, and standard deviation of the vertical plume profile, σ_z, for ground reflections and also a function of boundary layer depth, A, for boundary layer top reflections). Thus values of σ_z detailed in Figure 8 in Clarke (1979), depict the Gaussian distribution of σ_z assuming no reflections of activity off the ground (and the boundary layer top). For a fair comparison between R91 and NAME, σ_z accounting for the reflection of activity off the ground in R91 must be calculated.

Equations B1 and B2 detailed in this study (or alternatively Equation 4 in Clarke (1979)) consider the plume to be reflected off both the ground and the boundary layer. In this study no account has been made of the reflections off the boundary layer when calculating σ_z. This is deemed to be a valid assumption for the baseline scenario (ie, a low level release, in Pasquill stability category D conditions, for relatively short distances downwind). Figures 4-6 in the main text indicate that the main body of the plume does not reach the boundary layer top (800 m above ground level) until 10’s km downwind and therefore the contribution from reflections off the boundary layer top over the same downwind extent will be limited.

The distribution in the TIACs is described by a full Gaussian curve in the cross-wind direction in R91. The normalised concentration of this curve is:

$$C(z) = \frac{2}{\sqrt{2\pi}\sigma_{z,unreflected}} e^{\left(\frac{-z^2}{2\sigma^2_{z,unreflected}}\right)} \qquad \text{C4}$$

The factor of 2 increase in C(z) is due to the TIACs spreading through effectively half the Gaussian curve.

Equations C2 and C3 apply in the same manner to σ_z and the mean of z (the mean value of the vertical (z) co-ordinate), respectively. The mean of z for a reflected plume is estimated as detailed by Equations C5-C7.

$$\bar{z} = \int_0^\infty \frac{2z}{\sqrt{2\pi}\sigma_{z,unreflected}} e^{\left(\frac{-z^2}{2\sigma^2_{z,unreflected}}\right)} dz \qquad \text{C5}$$

There is no requirement to divide Equation C5 by the integral of C(z) with respect to z (as in Equation C3) because the concentration considered is normalised, ie, includes the factor 2/(((2π)^0.5)σ_z).

$$\bar{z} = \left[\frac{-2\sigma_{z,unreflected}}{\sqrt{2\pi}} e^{\left(\frac{-z^2}{2\sigma^2_{z,unreflected}}\right)} \right]_0^\infty \qquad \text{C6}$$

$$\bar{z} = \sqrt{\frac{2}{\pi}}\sigma_{z,unreflected} \qquad \text{C7}$$

The vertical standard deviation of the reflected plume is estimated as detailed by Equation C8.

$$\sigma^2_{z,reflected} = \int_0^\infty \frac{2\left(z-\bar{z}\right)^2}{\sqrt{2\pi}\sigma_{z,unreflected}} e^{\left(\frac{-z^2}{2\sigma^2_{z,unreflected}}\right)} dz \qquad \text{C8}$$

$$\sum C_i\left(z_i-\bar{z}\right)^2 = \sum C_i z_i^2 - 2\bar{z}\sum C_i z_i + \bar{z}^2 \qquad \text{C9}$$

$$\sum C_i\left(z_i-\bar{z}\right)^2 = \sum C_i z_i^2 - 2\bar{z}^2 + \bar{z}^2 \qquad \text{C10}$$

Equation C9 can be manipulated to the form of Equation C10 with the aid of Equation C5, which demonstrates that the mean of z is equal to the sum of each component of the concentration multiplied by the respective vertical co-ordinate. Equation C10 can then be used in the manipulation of Equation C8 to Equation C11.

$$\sigma^2_{z,\mathrm{reflected}} = \int_0^\infty \frac{2z^2}{\sqrt{2\pi}\sigma_{z,\mathrm{unreflected}}} e^{\left(\frac{-z^2}{2\sigma^2_{z,\mathrm{unreflected}}}\right)} dz - \bar{z}^2 \qquad \text{C11}$$

$$\sigma^2_{z,\mathrm{reflected}} = \int_0^\infty \frac{-2z\sigma_{z,\mathrm{unreflected}}}{\sqrt{2\pi}} \frac{(-z)}{\sigma^2_{z,\mathrm{unreflected}}} e^{\left(\frac{-z^2}{2\sigma^2_{z,\mathrm{unreflected}}}\right)} dz - \bar{z}^2 \qquad \text{C12}$$

Equation C11 is converted to Equation C12 to enable the integration (by parts) of the integral, detailed in Equations C13-C16.

$$\sigma^2_{z,\mathrm{reflected}} = \left[\frac{-2z\sigma_{z,\mathrm{unreflected}}}{\sqrt{2\pi}} e^{\left(\frac{-z^2}{2\sigma^2_{z,\mathrm{unreflected}}}\right)}\right]_0^\infty - \int_0^\infty \frac{-2\sigma_{z,\mathrm{unreflected}}}{\sqrt{2\pi}} e^{\left(\frac{-z^2}{2\sigma^2_{z,\mathrm{unreflected}}}\right)} dz - \bar{z}^2 \qquad \text{C13}$$

$$\sigma^2_{z,\mathrm{reflected}} = 2\sigma^2_{z,\mathrm{unreflected}} \int_0^\infty \frac{1}{\sqrt{2\pi}\sigma_{z,\mathrm{unreflected}}} e^{\left(\frac{-z^2}{2\sigma^2_{z,\mathrm{unreflected}}}\right)} dz - \bar{z}^2 \qquad \text{C14}$$

The integral in Equation 14 is integrated from 0 to infinity. This integral scaled by 2 is equivalent to a single integral integrated from minus infinity to infinity, as demonstrated by Equation C15. The integral in Equation C15 is akin to integrating over a full Gaussian profile, which equates to 1, hence Equation C16.

$$\sigma^2_{z,\mathrm{reflected}} = \sigma^2_{z,\mathrm{unreflected}} \int_{-\infty}^\infty \frac{1}{\sqrt{2\pi}\sigma_{z,\mathrm{unreflected}}} e^{\left(\frac{-z^2}{2\sigma^2_{z,\mathrm{unreflected}}}\right)} dz - \bar{z}^2 \qquad \text{C15}$$

$$\sigma^2_{z,\mathrm{reflected}} = \sigma^2_{z,\mathrm{unreflected}} - \bar{z}^2 \qquad \text{C16}$$

$$\sigma^2_{z,\mathrm{reflected}} = \sigma^2_{z,\mathrm{unreflected}}\left(1-\frac{2}{\pi}\right) \qquad \text{C17}$$

Equation C17 is derived by substituting Equation C7 into Equation C16. Thus the square of σ_z detailed in Figure 8 of Clarke (1979) must be scaled by 1-(2/π) to calculate σ_z accounting for the impaction of the plume on the ground and to enable comparison with σ_z calculated from NAME output.

References

Clarke RH (1979). The first report of a Working Group on Atmospheric Dispersion: a model for short and medium range dispersion of radionuclides released to the atmosphere. Chilton, NRPB-R91.

APPENDIX D

Estimating the vertical standard deviation of the plume for a uniform distribution across the boundary layer

Table 5 in the main text of this report highlights the standard deviation of the vertical plume profile, σ_z, as a function of distance downwind for both R91 and NAME model output. It is evident that only at the greatest distance downwind considered in this study (40 km) is the plume relatively uniformly distributed across the (800 m deep) boundary layer. This appendix explains how the value of σ_z is estimated for a plume uniformly distributed across the boundary layer.

As seen previously in this report the vertical standard deviation of the plume is described by Equation D1 and the mean value of the vertical (z) co-ordinate is described by Equation D2.

$$\sigma_z^2 = \frac{\int (z-\bar{z})^2 C(z)dz}{\int C(z)dz} \qquad \text{D1}$$

$$\bar{z} = \frac{\int zC(z)dz}{\int C(z)dz} \qquad \text{D2}$$

It is assumed that the vertical TIAC profile is uniform such that C(z) = 1/h, for 0 < z < h, and C(z) = 0 elsewhere (where h is the depth of the boundary layer). The derivation of a method for estimating the mean value of the vertical (z) co-ordinate for a plume uniformly distributed across the boundary layer is detailed in equations D3 and D4.

$$\bar{z} = \frac{\int_0^h \frac{z}{h}dz}{\int_0^h \frac{1}{h}dz} \qquad \text{D3}$$

$$\bar{z} = \frac{h}{2} \qquad \text{D4}$$

$$\sigma_z^2 = \frac{\int_0^h \left(z - \bar{z}\right)^2 \frac{1}{h} dz}{\int_0^h \frac{1}{h} dz} \qquad \text{D5}$$

$$\sigma_z = \sqrt{\frac{h^2}{12}} \qquad \text{D6}$$

The derivation of a method for estimating the vertical standard deviation of a plume uniformly distributed across the boundary layer is detailed in equations D5 and D6. 'h/2' derived in Equation D4 is used to replace the mean value of the vertical (z) co-ordinate of a plume in Equation D5. For a boundary layer depth of 800 m, σ_z = 231 m.